



SAPIENZA
Università di Roma
Facoltà di Scienze Matematiche Fisiche e Naturali

DOTTORATO DI RICERCA
IN GENETICA E BIOLOGIA MOLECOLARE

XXIV Ciclo
(A.A. 2010/2011)

**Functional characterization of genes that control structure and
dynamics of centrosomes in *Drosophila***

Dottoranda
Ramona Lattao

Docente guida
Prof.ssa Silvia Bonaccorsi

Tutor
Dott.ssa Patrizia Lavia

Coordinatore
Prof.ssa Irene Bozzoni

Ramona Lattao

***Cover image:** primary spermatocyte centrioles from *Drosophila* wild type testes immunostained with anti-DSpd-2 (green) and anti-Fract (red). (R. Lattao)*

INDEX

| | |
|--|-----------|
| GLOSSARY | 5 |
| SUMMARY | 9 |
| 1. INTRODUCTION | 11 |
| 1.1 THE CELL CYCLE | 11 |
| 1.1.1. <i>Cell-cycle control system</i> | 12 |
| 1.2 THE SPINDLE | 13 |
| 1.2.1. <i>Microtubules (MTs)</i> | 14 |
| 1.2.2. <i>Microtubule-organizing centers (MTOCs)</i> | 16 |
| 1.2.3. <i>The centrosome</i> | 16 |
| 1.2.4. <i>The centriole</i> | 18 |
| 1.2.5. <i>Centrosome and centriole duplication</i> | 19 |
| 1.2.6. <i>Bipolar spindle assembly</i> | 25 |
| 1.2.7. <i>Spindle size</i> | 29 |
| 1.3. <i>DROSOPHILA MELANOGASTER</i> AS MODEL SYSTEM TO STUDY CELL DIVISION | 30 |
| 1.3.1. <i>Drosophila male meiosis</i> | 31 |
| 2. AIMS | 35 |
| 3. RESULTS AND DISCUSSION..... | 37 |
| 3.1 CHARACTERIZATION OF <i>DROSOPHILA</i> MALE MEIOTIC SPINDLES ... | 37 |
| 3.2 GENERATION OF NEW <i>Tb</i> -MARKED BALANCER CHROMOSOMES.... | 45 |
| 3.3 IDENTIFICATION OF <i>DROSOPHILA</i> GENES REQUIRED FOR MALE MEIOSIS BY A CYTOLOGICAL SCREEN OF MALE-STERILE AND LETHAL MUTANTS. | 48 |
| 3.4 <i>MOST</i> | 49 |
| 3.4.1. <i>Cytological characterization of mutant phenotype</i> | 49 |
| 3.4.2. <i>Gene cloning</i> | 51 |
| 3.5 <i>FRACT</i> | 55 |
| 3.5.1. <i>Cytological characterization of mutant phenotype</i> | 55 |
| 3.5.2. <i>Gene cloning</i> | 57 |
| 3.5.3. <i>Subcellular localization of Fract</i> | 58 |
| 3.5.4. <i>Conclusions and perspectives</i> | 64 |

| | |
|---|-----------|
| 4. MATERIALS AND METHODS..... | 67 |
| 4.1 <i>DROSOPHILA</i> STRAINS | 67 |
| 4.2 CYTOLOGY | 67 |
| 4.2.1. <i>In vivo time lapse video microscopy</i> | 68 |
| 4.2.2. <i>X-Gal Staining</i> | 68 |
| 4.2.3. <i>S2 cells transfection and staining</i> | 69 |
| 4.2.4. <i>Axial Ratio (A.R.) determination</i> | 69 |
| 4.2.5. <i>Spindle and aster measurement</i> | 69 |
| 4.2.6. <i>Statistical analysis</i> | 70 |
| 4.3 MOLECULAR BIOLOGY | 70 |
| 4.3.1. <i>Genomic DNA extraction</i> | 70 |
| 4.3.2. <i>RNA extraction and RT-PCR</i> | 70 |
| 4.4 BIOCHEMISTRY | 71 |
| 4.4.1. <i>Antibody induction and purification</i> | 71 |
| 4.4.2. <i>Western blot</i> | 72 |
| REFERENCES..... | 73 |
| LIST OF PUBLICATIONS..... | 95 |
| ACKNOWLEDGEMENT | 97 |

GLOSSARY

Astral microtubules: a subpopulation of microtubules nucleated at the centrosome that radiate outward and contact the cell cortex; they are involved in spindle positioning.

Axoneme: the microtubule-based structure within cilia and flagella that gives them rigidity and the ability to move. It is a cylindrical structure comprised of nine pairs of doublet microtubules, arranged around a central pair of single microtubules (9+2). The central microtubules can be absent in non-motile cilia (9+0).

Balancer: chromosome with multiple inversions that suppress recombination and allows genetic stability of a mutant stocks. It carries dominant markers to distinguish homozygous and heterozygous flies.

Basal body: structure found at the base of eukaryotic cilia and flagella that organizes the assembly of the axoneme. Centrioles can give rise to basal bodies and *vice versa*. Basal body and centriole share the same structure; additionally, basal bodies have a transition zone at their distal end, which is contiguous with the axoneme.

Cartwheel structure: a basal body precursor and one of the first structures to appear during basal body formation. It consists of a central hub and nine spokes, on top of which microtubules are added.

Cell-cycle checkpoints: molecular mechanisms that monitor cell-cycle progression, ensuring that genome replication (S phase) and segregation (mitosis) take place in an ordered fashion. Checkpoints act to delay Cdk activation until conditions are met, or induce apoptosis in the presence of irreparable damage or high levels of stress. Checkpoints include the DNA damage checkpoint (three points in cell cycle: G1, intra-S and G2–M), stress responses (G1 and G2) and the spindle assembly checkpoint in mitosis.

Centrioles: the canonical centriole is a cylinder that is comprised of nine microtubule triplets; it is variable in length and has

appendages at its distal ends upon maturation. There are variations of this structure, in which triplets are substituted by singlets or doublets and there are no appendages. Centrioles are also important for the formation and maintenance of the cilium.

Centriole disengagement: loss of the orthogonal orientation of the two centrioles of a centrosome at the end of mitosis and beginning of the G1 phase. This event precedes new centriole formation.

Centrosomes: specialized organelles consisting of a pair of centrioles surrounded by an electron-dense matrix, the pericentriolar material (PCM). The centrosome is the primary microtubule organizing centre (MTOC) in animal cells, centrosomes nucleate and organize microtubules and forms the spindle poles during mitosis.

Cilium: slender cellular projections that extend up to 10 μm outwards from the cell and contain an axoneme. The majority of vertebrate cells have cilia. Cells can have motile or non-motile (primary) cilia. Cilia can serve as sensory organelles or, in the case of motile cilia, can move fluids around the cell. Motility is thought to depend on the structure of the axoneme, with most motile cilia displaying a 9+2 axoneme structure.

Core promoter recognition factor: a protein or multi-subunit complex that binds with sequence specificity to core promoter elements. The prototypical core promoter recognition factor for mRNA genes in eukaryotes is transcription factor IID (TFIID), whose subunits recognize multiple core promoter elements.

Cyclin-dependent kinases (Cdks): family of serine/threonine kinases activated by association with specific cyclins. Cell-cycle progression is controlled by a number of cyclin-Cdk complexes. Entry into G1 in response to mitogenic signals is governed mostly by cyclin-D-Cdk complexes. The sequential activation of cyclin-E-Cdk2 and cyclin-A-Cdk2 complexes promotes G1 to S transition and S-phase progression, whereas activation of cyclin-A-Cdk1 and cyclin-B-Cdk1 complexes facilitates entry into mitosis.

Flagella: axoneme (9+2) MT-based cellular projections that help propel cells.

Kinetochores: multiprotein complex that assembles on centromeric DNA. Kinetochores mediate microtubule attachment to chromosomes during mitosis.

Microtubule (MT): a hollow tube, 25 nm in diameter, formed by the lateral association of 13 protofilaments. Each protofilament is a polymer of α - and β -tubulin subunits.

Pericentriolar material (PCM): a proteinaceous matrix that surrounds centrioles in the centrosome; PCM mediates MT nucleation.

Polo-like kinases (Plks): a family of cell-cycle-regulated mitotic serine/threonine kinases (four members in mammals) with important roles in centrosome duplication, centrosome maturation, mitotic spindle function and cytokinesis.

RNA polymerase II (RNAPII): the enzyme that synthesizes mRNA in eukaryotic cells. RNAPII is composed of 12 protein subunits (RPB1–RPB12). The binding of RNAPII to promoters and the initiation of transcription requires many general transcription factors (TFs), for example, TFIIA, TFIIB, TFIID, TFIIIE, TFIIF and TFIIH.

Spindle: bipolar array of microtubules that mediates chromosome segregation.

Spindle assembly checkpoint (SAC): a monitoring system that prevents anaphase onset until all chromosomes are bi-oriented on the metaphase plate. The checkpoint function is performed by a protein complex that resides on kinetochores. Disrupting members of the SAC protein complex generates chromosome instability in cells and organisms.

Spindle pole body: the microtubule-organizing centre of yeast and diatoms. It is a plaque-like structure that is embedded in the nuclear membrane. It nucleates microtubules both on the cytoplasmic and nuclear side.

Transcription factor IID (TFIID): a transcription factor for RNA polymerase II that binds core promoters. The TFIID complex is

composed of the TATA-box-binding protein (TBP) and 13 or 14 TBP-associated factors.

TATA-box-binding protein (TBP): the central subunit of transcription factor IID (TFIID). TBP binds TATA boxes found in the core promoters of some eukaryotic mRNA genes.

TBP-associated factor (TAF): All subunits of the transcription factor IID (TFIID) complex other than the TATA-box-binding protein (TBP) are TAFs. There are 13 or 14 TAFs in the prototypical TFIID complex. There are also several proteins with sequence similarity to the prototypical TAFs, which are referred to as non-prototypical TAFs.

TBP-related factor (TRF): a protein that is highly related in sequence to TATA-box-binding protein (TBP).

WD domain: 44–60 residue sequence unit that typically contains the GH dipeptide (11–24 residues) at its N-terminus and the WD dipeptide at its C-terminus. Each WD40 repeat comprises a four-stranded antiparallel β -sheet. The conserved residues of the domain form a strong hydrogen bond network and stabilize the WD40 repeat fold. WD40 domain-containing proteins are very abundant in eukaryotic organisms, and are rarely present in prokaryotes.

SUMMARY

The general aim of my PhD thesis work was the characterization of *Drosophila* male meiosis, a widely used model system for genetic and molecular dissection of cell division. I first asked why the meiotic spindle of *Drosophila* males is much larger than the female meiotic spindle or the mitotic spindles of various cell types. I hypothesized that such large size reflects the availability of a large amount of tubulin stored in spermatocytes to be used postmeiotically for sperm tail assembly. To test this hypothesis, I examined male meiosis in 6 *Drosophila* species with dramatically different sperm flagella, ranging in length from 0.3 mm in *D. persimilis* to 58.3 mm in *D. bifurca*. I found that males of different species exhibit striking variations in meiotic spindle size, which positively correlate with sperm length, with *D. bifurca* showing a 30-fold larger spindle than *D. persimilis*. This suggests that primary spermatocytes of *Drosophila* species manufacture and store amounts of tubulin that are proportional to the length of the sperm tail and use these tubulin pools for spindle assembly. My findings also highlight an unsuspected plasticity of the meiotic spindle and suggest that the fidelity of chromosome segregation is largely independent of spindle size (Lattao et al. 2012, in press).

I also performed a screen aimed at the identification of new *D. melanogaster* genes controlling centrosome structure and/or behavior. To facilitate this screen I developed two novel *Tubby*-marked balancer chromosomes that allow unambiguous recognition of mutant larvae from their heterozygous non-mutant siblings (Lattao et al., 2011). My screen led to the isolation of two mutants with abnormal numbers of centrosomes: *multi asters* (*most*) and *fragile centrioles* (*fract*). I characterized the meiotic phenotypes of these mutants and cloned the genes they specify. *most* encodes 749 aa transcription factor of the TFIID superfamily, with homology with the TBP-related factors. Mutations in *most* cause an arrest in the first meiotic

prometaphase/metaphase and often exhibit multiple centrosomes in the aberrant meiotic figures. Thus, *most* belongs to a class of genes collectively known as meiotic arrest genes. These genes identify two independent pathways required for meiotic progression and spermatid differentiation. Gene expression analyses allowed definition of the *most* function, suggesting that it regulates the translation of *twine* (*cdc25*) mRNA, without affecting the spermatid differentiation pathway. My results also suggest that the centrosome phenotype of *most* mutants is likely to be an indirect consequence of meiotic arrest.

Cytological analysis showed that premeiotic spermatocytes of *fract* mutants display 2 centrioles at each cell pole. However, meiotic ana-telophase I figures of the same mutants often exhibit two regular centrioles at one cell pole but only one at the opposite pole, suggesting that *fract* is required for centriole stability during the meiotic division. *fract* encodes a 322 aa testis-specific protein that contains WD repeats. The EMS-induced *fract*^l mutant allele I characterized carries a stop codon that truncates the Fract protein into a 298 aa polypeptide. A polyclonal antibody raised against Fract decorates the distal end of male meiotic centrioles. This specific staining pattern is lost in *fract* mutants, where the antibody decorates the entire centriole, suggesting that the C-terminal region of Fract is crucial for its correct localization. Collectively, these results strongly suggest that *fract* does not play an essential role in centriole duplication or assembly but it is instead required for the maintenance of centriole integrity during male meiosis, a function never described in other organisms.

1. INTRODUCTION

1.1 The cell cycle

A cell reproduces by performing an orderly sequence of events in which it duplicates its contents and then divides into two. This cycle of duplication and division, known as the cell cycle, is the essential mechanism by which all living cells reproduce. The details of the cell cycle vary among organisms but some features are universal. The fundamental task of the cell cycle is the transmission of the genetic information to the next generation of cells. The DNA must be first faithfully replicated and then be accurately segregated to two daughter cells. In addition, during the cell cycle, cells also duplicate their organelles and macromolecules.

The cell cycle is divided into two major periods: interphase and M phase. Interphase consists of two gap phases called G_1 and G_2 , separated by an S phase during which DNA and organelles are duplicated in order to allow the production of two identical daughter cells. The M phase comprises two major events: the nuclear division, or mitosis, during which the chromosomes are distributed to the daughter nuclei; and the cytoplasmic division or cytokinesis when the cell itself divides into two. Generally, mitosis is subdivided into four phases: prophase, metaphase, anaphase and telophase. During prophase the DNA molecules condense into chromosomes consisting of two sister chromatids, which remain linked together through the action of specific cohesion proteins. When the nuclear envelope disassembles, the sister chromatids pairs become attached to a spindle-shaped bipolar array of microtubules (the mitotic spindle) through specialized structures called kinetochores. Sister chromatids attach to opposite poles of the spindle and align at the spindle equator during metaphase. At anaphase the sister-chromatid cohesion is disrupted and the sister-chromatids are pulled towards opposite poles of the spindle.

During telophase, a dense array of microtubules called central spindle assembles at the equator of the dividing cell. In correspondence of the central spindle midzone the cell forms a contractile ring. This structure assembles just beneath the plasma membrane and contains actin filaments, myosin II filaments and many structural and regulatory proteins. During telophase the contractile ring gradually constricts concomitant to membrane addition to the cell equator. When ring contraction is completed, the gap between the daughter cells is sealed; at the same time the spindle disassembles and the segregated chromosomes are packaged into daughter nuclei.

1.1.1. Cell-cycle control system

The cell cycle is regulated by a control system that is based on a connected series of biochemical switches, each of which initiates a specific event. In most eukaryotic cells, this control system triggers the cell-cycle progression at three major regulatory transitions or checkpoints. The first checkpoint, called Start or restriction point, is in late G₁ and regulates the commitment of the cell to enter the cycle and duplicate the DNA. The second is the G₂/M checkpoint that controls the early mitotic events that ultimately lead to metaphase. The third is the spindle checkpoint that regulates the metaphase-to-anaphase transition, allowing completion of mitosis and cytokinesis. The cell cycle control system blocks progression through each of these checkpoints if it detects problems inside or outside the cell.

Central mediators of the cell-cycle control are members of a family of kinases known as cyclin-dependent kinases (Cdks). The activity of these kinases rises and falls as the cell progresses through the cycle, leading to cyclic changes in the phosphorylation of proteins that initiate or regulate cell cycle events. Cyclical changes in Cdk activity are regulated by cyclins; these proteins were originally named cyclins because they undergo a cycle of synthesis and degradation at each cell cycle. The levels of Cdks, by contrast, are constant, at least in the simplest cell cycles. Cyclical

changes in cyclin levels result in the cyclic assembly and activation of the cyclin-Cdk complexes, which in turn trigger cell-cycle events. Each cyclin does not simply activate its Cdk partner but also directs it to specific target proteins. There are four classes of cyclins, each defined by the stage of the cell cycle at which they bind Cdks and function. G₁/S cyclins activate Cdks in late G₁ and help cells to progress through the Start. S cyclins help stimulating chromosome duplication. Their levels remain elevated until mitosis and also contribute to the control of some early mitotic events. M cyclins stimulate entry into mitosis at the G₂/M checkpoint and are degraded in mid-mitosis. G₁ cyclins do not oscillate during the cell cycle like the other cyclins; they coordinate cell growth with the entry to a new cell cycle and help the activity of G₁/S cyclins.

In yeast, a single Cdk protein triggers different cell-cycle events by changing cyclin partners at different stages of the cycle. In vertebrates, by contrast, there are four Cdks. Full activation of the cyclin-Cdk complex requires an additional kinase, called Cdk-activating kinase (CAK), which phosphorylates a site on Cdk causing a small conformational change. The rise and fall of cyclin levels is the primary determinant of Cdk activity but several additional mechanisms tune Cdk activity at specific stages of the cycle. Phosphorylation of Cdk by the protein kinase Wee1 inhibits Cdk activity, while its dephosphorylation by the Cdc25 phosphatase increase Cdk activity. Binding of Cdk inhibitor proteins (CKIs) also regulates cyclin-Cdk complexes.

1.2 The spindle

Mitosis is mediated by the spindle, a bipolar array of microtubules (MTs) associated with several proteins including motor proteins that travel along the MTs. The spindle is a complex molecular machinery that mediates chromosome alignment at the cell equator and then sister chromatid movement during anaphase, thereby segregating the two sets of chromosomes to the opposite

ends of the cell where they are packaged into daughter nuclei (Fig. 1) (reviewed in O'Connell and Khodjakov, 2007; Walczak and Heald, 2008; Dumont and Mitchison, 2009). The mitosis-related process meiosis uses a similar molecular machine, the meiotic spindle, to reduce the size of the genome by half during the generation of haploid gametes. Consequently, the actions of the mitotic and meiotic spindles are crucial for the formation, maintenance and reproduction of healthy organisms.

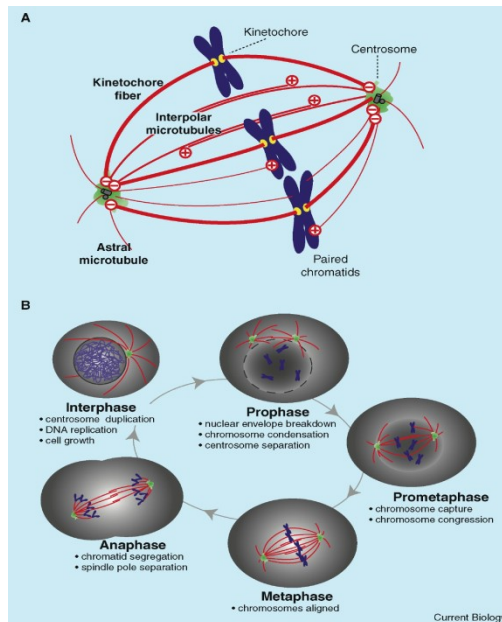


Figure 1. (A) Main components of the metaphase mitotic spindle. **(B)** The stages of mitosis illustrating microtubule reorganization and chromosome translocation. (from Gadde and Heald, 2004)

1.2.1. Microtubules (MTs)

MTs are highly dynamic polymers that switch between cycles of growth and depolymerization. MTs are long, hollow cylinders with an outer diameter of 25 nm that are assembled from α -tubulin and β -tubulin heterodimers in a GTP-dependent manner. A microtubule consists of 13 parallel protofilaments, each composed of

alternating α -tubulin and β -tubulin molecules. This structure makes MTs stiff and difficult to bend. The subunits in each protofilament all point to the same direction, and the protofilaments themselves are aligned in parallel. Therefore, the MT has a structural polarity: the α -tubulin subunits are exposed at the MT minus end, while the β -tubulin subunits are exposed at its plus end.

Microtubule nucleation largely depends on γ -tubulin, an evolutionary conserved member of the tubulin super-family that shares 30% homology with α -tubulin and β -tubulin (Oakley and Oakley, 1989). γ -tubulin is part of a highly conserved multi-protein complex first identified in centrosomes isolated from *Drosophila* embryos (Raff et al., 1993; Moritz et al., 1998) and found to form 25 nm open ring structures designated as γ -tubulin ring complexes (γ TuRCs) (Zheng et al., 1995). γ TuRCs are capable of nucleating MTs *in vitro* (Stearns and Kirschner, 1994); they are composed of 13 γ -tubulin subunits as well as numerous γ -tubulin complex protein (GCPs) or γ TuRC-interacting proteins (GRIPs). The γ TuRC dissociates under high salt conditions to yield a stable subcomplex of two molecules of γ -tubulin associated with two GCPs which is called γ -tubulin small complex (γ TuSC) (Oegema et al., 1999). The γ TuSC is the conserved, essential core of the microtubule nucleating machinery and is found in nearly all eukaryotes (reviewed in Kollman et al., 2011).

In the mitotic spindle, MTs are oriented with their minus end focused at the spindle poles and the plus end outward from the poles. The spindle MTs are generally classified into three types: interpolar microtubules, kinetochore microtubules and astral microtubules. The plus ends of the interpolar microtubules emanating from the opposite poles interact to each other, resulting in an antiparallel array at the spindle midzone. The plus ends of kinetochore microtubules are embedded into a large protein assembly called kinetochore located at the centromere of each sister chromatid. Finally, astral microtubules radiate outward from the poles and contact the cell cortex, helping the positioning of the spindle in the cell.

1.2.2. Microtubule-organizing centers (MTOCs)

MTs are generally nucleated from specific intracellular sites known as MT-organizing centers (MTOCs). Microtubules are nucleated at their minus end, with the plus end growing outward from each MTOC. More than a century ago, the centrosome was identified as the primary MTOC in animal cells (Boveri, 1914). In fungi, the functional analogue of the centrosome is the spindle pole body, which is a large multilayered structure embedded in the nuclear envelope that nucleates MTs on both cytoplasmic and nuclear face (reviewed in Jaspersen and Winey, 2004). Plants, on the other hand, have no centrosome equivalent, but they nevertheless have highly organized acentrosomal MT arrays (Wasteney and Ambrose, 2009). Acentrosomal MTs are also produced in animal cells; these MTs are nucleated around the chromosomes and are essential for spindle formation in both centrosome-containing cells and in cells devoid of centrosomes such as the female oocytes (O'Connell and Khodjakov, 2007; Walczak and Heald, 2008; Dumont and Mitchison, 2009; Mottier-Pavie et al., 2011).

1.2.3. The centrosome

The centrosome is an organelle composed of a pair of MT-based centrioles surrounded by a pericentriolar matrix (PCM). The PCM has been visualized as a fibrous lattice (Dictenberg et al., 1998) and, in a human centrosome, contains over 100 different proteins including γ -tubulin and associated proteins (Andersen et al., 2003).

Centrosomes determine the geometry of MT arrays throughout the cell cycle, and thus they play roles in cell shape determination, polarity and motility, as well as in spindle formation and chromosome segregation (reviewed Luders and Stearns, 2007). Importantly, centrioles also function as basal bodies for the formation of cilia and flagella (Fig. 2).

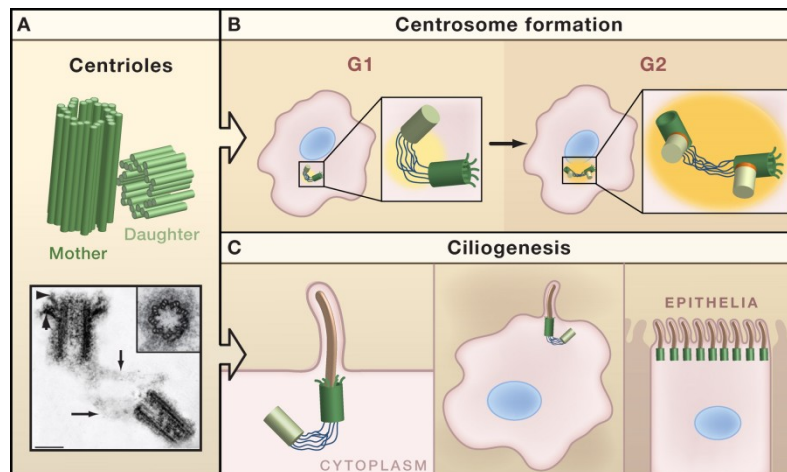


Figure 2 (A) A centriole pair is shown schematically and as seen by electron microscopy (EM) Scale bar = 0.2 μm . In the EM image the mother centriole can be distinguished by two types of appendages at its distal end (thick arrow points to subdistal appendages, arrowhead to distal appendages). The centrioles are “disengaged,” although they remain linked by a fibrous network (arrows). The inset shows a cross-section through a centriole barrel. **(B)** In actively proliferating cells, the centrioles organize a PCM (yellow) to form a centrosome. **(C)** In many cells that are not actively proliferating, the centrosome migrates to the cell surface and a cilium (brown) is assembled from the mother centriole. In certain epithelial cells, many centrioles are assembled at once leading to the formation of multiciliated cells. (from Nigg and Raff, 2009)

Many cell cycle regulatory proteins are enriched at the centrosome and depletion of some centrosome components was shown to arrest cells in G1/S-phase, suggesting that the integrity of the centrosome is essential for cell cycle progression (Mikule et al., 2007), at least in some model systems.

In vertebrate cycling cells, the amount of PCM associated with the centrioles varies throughout the cell cycle. In S-phase, the PCM, the MT nucleation and MT-anchoring capacities of the centrosome are at their lowest levels (Piehl et al., 2004). Before mitosis, centrosomes “mature” by accumulating more PCM, and in late prophase-prometaphase, the PCM levels reach a maximum level. Consequently, MT-nucleating and MT-anchoring activities

of these organelles are at their highest, allowing the formation of robust asters that morph into the bipolar mitotic spindle (Snyder and McIntosh, 1975; Kuriyama and Borisy, 1981).

Upon mitotic exit, PCM levels on centrosomes drop (Khodjakov and Rieder, 1999). Using an antibody that recognizes mitotic phosphoepitopes the phosphorylation and maturation cycles of the centrosome were found to perfectly match (Snyder and McIntosh, 1975; Kuriyama and Borisy, 1981; Rieder, 1982), suggesting that specific phosphorylation events lead to PCM recruitment during mitotic entry. In particular, two kinases were found to be important for centrosome maturation: Polo and Aurora A (Brittle and Ohkura, 2005; Glover, 2005; Barr and Gergely, 2007).

1.2.4. The centriole

Centrioles are barrel-shaped structures that lie orthogonal to each other and exhibit a highly conserved nine fold symmetry. They are generally formed by triplets of MTs but in some organisms centrioles can consist of nine doublets of MTs (e.g in *Drosophila*) or singlets (e.g in *Caenorhabditis elegans*) (Delattre and Gonczy, 2004). The centriole appeared very early in evolution and it was probably already present in the common ciliated unicellular ancestor of eukaryotes in the form of a basal body (Cavalier-Smith, 2002). Centrioles can give rise to the basal bodies of cilia: a centriole can migrate to the cell cortex, attach to the plasma membrane and initiate the assembly of a cilium. In mammalian cells the centriole-basal body conversion occurs during G1 (Wheatley et al., 1996).

At the ultra structural level, motile cilia exhibit a 9+2 structure, with 9 MT doublets surrounding a central MT pair (Gibbons, 1981). Electron microscopy studies carried out in the early 60's showed that a 9+0 structure (now termed primary cilium) was present in many differentiated mammalian tissues including the kidney, fibroblasts and neurons (Barnes, 1961; Sorokin, 1962). However, primary cilia were considered as vestigial organelles without any major cellular function for several decades (Satir and

Christensen, 2007). It was therefore surprising when several recent studies revealed the importance of primary cilia in key development events (Nonaka et al., 1998) and their involvement in several signaling pathways in vertebrates (Huangfu et al., 2003; Gerdes et al., 2009; Veland et al., 2009).

Since protein biosynthesis does not take place inside the cilium, the assembly of this structure entirely relies on the transport of proteins along the axoneme, a process known as intraflagellar transport (IFT) (Scholey and Anderson, 2006; Blacque et al., 2008). The combination of proteomic approaches and bioinformatic analyses that compared the genomes of ciliated and non-ciliated organisms produced a comprehensive list of centriole and cilia components (Andersen et al., 2003; Avidor-Reiss et al., 2004; Broadhead et al., 2006; Kilburn et al., 2007). These studies estimated that the vertebrate cilium might require up to 1000 polypeptides for its assembly and function (Ostrowski et al., 2002; Pazour, 2004; Pazour et al., 2005; Gherman et al., 2006). The results of these systematic approaches to cilia composition allowed identification of many human diseases with cilia defects, defining a new group of human diseases: the ciliopathies (Badano et al., 2006; Hildebrandt et al., 2011).

1.2.5. Centrosome and centriole duplication

Centrosome duplication is intimately coupled to cell cycle: the conclusion of each cell cycle culminates in the production of two genetically identical cells, each receiving a single copy of the genome and a single centrosome.

The centrosome cycle can be subdivided into distinct steps: centriole disengagement, centriole duplication, centrosome maturation, and centrosome separation (reviewed in Nigg, 2007). In a metaphase cell each spindle pole is characterized by the presence of one centrosome comprising two centrioles. These two centrioles represent a parent-progeny pair originating from the previous cell cycle; they are tightly associated with each other and usually have an orthogonal arrangement. The tight link between

the two centrioles is lost upon exit from the M phase or during early G₁ in a process referred to as “disengagement”. This process is proposed to license the two centrioles for a new round of duplication (Tsou and Stearns, 2006b) and involves the protease separase and the Polo-like kinase 1 (Plk1) (Tsou and Stearns, 2006b; Tsou and Stearns, 2006a). During the S phase one new centriole called procentriole begins to grow at an orthogonal angle next to each licensed centriole. Once the assembly of the two new procentrioles has initiated, further centriole duplication is inhibited until the cell passes through mitosis (Wong and Stearns, 2003). The two procentrioles then elongate until they reach full length in G₂. In late G₂, the younger centriole of the parental pair acquires appendages, thereby reaching full maturity. At about the same time, the loose tether between the two parental centrioles is severed to enable centrosome separation. When centrioles are absent, new centrioles can form *de novo*, suggesting that the role of preexisting centrioles is not to template the centrioles but rather to bias the spatial location where the procentriole assembles (Rodrigues-Martins et al., 2007a).

Genetic studies and RNAi-based screens have identified five centrosome/centriole-associated proteins required for centrosome duplication in *C. elegans*: the protein kinase ZYG-1, as well as the SAS-4, SAS-5, SAS-6 and SPD-2 proteins characterized by coiled-coil domains (O'Connell et al., 2001; Kirkham et al., 2003; Leidel and Gonczy, 2003; Kemp et al., 2004; Pelletier et al., 2004; Leidel et al., 2005). These five proteins act sequentially during centriole biogenesis (Dammermann et al., 2004); after fertilization of *C. elegans* eggs, SPD-2 is initially recruited to the paternal centriole where it is required for localization of ZYG-1, which is in turn required for recruitment of SAS-5 and SAS-6, and then SAS-4. Electron tomography studies showed that centriole assembly in *C. elegans* involves the SAS-5 and SAS-6-dependent formation of a central tube followed by a SAS-4-dependent assembly of MTs onto the periphery of the tube (Pelletier et al., 2006). SPD-2, SAS-4 and SAS-6 all have homologues in both humans and *Drosophila*:

the human homologues are termed Cep192 (Andersen et al., 2003), CPAP (Hung et al., 2000) and hSAS-6 (Leidel et al., 2005), respectively. Recently, a protein called Ana2 was shown to be the likely orthologue of SAS-5 in *Drosophila*; Ana2 interacts with DSAS-6 and it is essential for centriole duplication (Stevens et al., 2010). The human orthologue of Ana2 is STIL or SIL and has been shown to be essential for proper mitotic spindle assembly (Pfaff et al., 2007; Kumar et al., 2009). There are no obvious homologues of ZYG-1 in the human and fly genomes, but the human Plk4 kinase and its *Drosophila* orthologue Sak might be the functional analogues of ZYG-1. Inhibition of Plk4 or Sak prevents centriole duplication, while overexpression of either protein leads to the assembly of supernumerary centrioles (Bettencourt-Dias et al., 2005; Habedanck et al., 2005). Studies on SPD-2 orthologues in humans and flies suggest that the primary function of these proteins is to recruit PCM around the centrioles (Gomez-Ferreria et al., 2007; Giansanti et al., 2008). *Drosophila* Asterless (Asl) and its related vertebrate protein Cep152 are instead PCM components that localize near the centrioles wall and are required for centriole duplication (Bonaccorsi et al., 1998; Varmark et al., 2007; Blachon et al., 2008).

Initiation of centriole assembly and establishment of the ninefold symmetry requires a structure called the cartwheel, which is located at the proximal end of centrioles and the basal bodies in a wide range of organisms. In vertebrates, a cartwheel structure is present at the base of procentrioles but is no longer seen in daughter and mother centrioles (Alvey, 1986). The cartwheel is formed by a central hub from which nine evenly spaced spokes emanate, terminated by a pinhead structure to which the MTs triplets attach. In *Chlamydomonas* two component of the cartwheel have been described: CrSas-6/Bld-12 and Bld10p. CrSas-6/Bld-12 is the homologue of SAS-6 and has been proposed to be part of the inner spokes or the hub of the cartwheel (Nakazawa et al., 2007). SAS-6 localizes to the central hub of the cartwheel also in *Drosophila* (Gopalakrishnan et al., 2010) suggesting that proteins

of the SAS-6 family are required to build the central hub and that this hub plays a role in establishing the ninefold symmetry (Rodrigues-Martins et al., 2007b).

Bld-10 has been shown to form the outer spoke and the pinhead structure in *Chlamydomonas* (Hiraki et al., 2007), controlling the length of the radial spokes and specifying centriole diameter. Cep135, the human orthologue of Bld10p, also localizes to the cartwheel and is essential for centriole assembly (Ohta et al., 2002). Bld10/Cep135 function is apparently dispensable for the initiation of centriole assembly in *Drosophila*. However, ultrastructural analysis has revealed that in the absence of Bld10/Cep135 sperm basal bodies are shorter than in wild type and most of the axonemes lack the central pair of MTs, leading to male sterility (Mottier-Pavie and Megraw, 2009).

Assembly of the centriole MT triplet seems to occur sequentially. Singlet MTs, or A-tubules, first attach to the spokes of the cartwheel then doublets and triplets (incomplete B and C-tubules, respectively) assemble (Guichard et al., 2010). In humans, in the nascent procentriole, the proximal or minus end of the A-tubule is capped by a conical structure resembling the γ -tubulin ring complex (γ -TURC). This suggests that each A-tubule is nucleated by a γ -TURC and then grows unidirectionally from the proximal to the distal end. In contrast, the incomplete B- and C-tubules are never capped at their proximal end, suggesting that their assembly is initiated by a different mechanism (Guichard et al., 2010). To date, there is still no mechanistic clue as to how the formation of the incomplete B- and C-tubules is achieved.

At the stage at which B- and C-tubules start to assemble, procentrioles are short, with their length slightly exceeding the length of the cartwheel (Loncarek et al., 2008). In the subsequent stages of assembly, procentrioles undergo elongation to eventually reach the full length. Centriole length appears to be under active control. This view is not only based on the limited variation in centriole length observed in any given cell type but also on the fact that centriole length undergoes dynamic changes at well-defined

stages in the assembly process. In mammalian proliferating cells, procentrioles assembled at the G1/S transition or during early S phase start to elongate during the S phase, and elongation proceeds further during G2 and mitosis (Vorobjev and Chentsov Yu, 1982). Centriole elongation seems to be coupled to cell-cycle progression. In mammalian cells arrested in S phase by drugs that inhibit DNA replication, procentrioles elongate to reach approximately 70% of the full length, which corresponds to the typical length of late S-phase procentrioles in untreated cells, but do not elongate further, suggesting that completion of centriole elongation requires transition into G2 (Rattner and Phillips, 1973). Centriole elongation can also be restricted to certain cell types or certain developmental stages, like in *Drosophila* flagella (Callaini et al., 1997).

Incorporation of tubulin dimers into centriolar MTs appears to occur beneath a distal cap containing the CP110 protein (Kleylein-Sohn et al., 2007). CP110 is conserved in animals and is essential for centriole duplication (Chen et al., 2002). CP110, together with another centriolar protein called Cep97, has also been implicated in the control of primary cilia formation in mammalian cells. The current model is that CPAP and CP110 are both involved in the control of centriole length. CPAP would promote elongation, possibly by favoring tubulin incorporation at the plus end of centriole MTs, whereas CP110 capping activity would limit microtubule growth (Schmidt et al., 2009).

More recently, another centriolar component called Ofd1 was found to play a role in controlling the length of mammalian centrioles (Singla et al., 2010). Ofd1 is a conserved centriolar protein known to be mutated in different types of ciliopathies (Keller et al., 2005). Ofd1 localizes to the distal ends of mother and daughter centrioles, as well as procentrioles. Interestingly, CP110 and Cep97 localization at the distal end of centrioles is unaffected by Ofd1 depletion, suggesting that these proteins act in a separate pathway for centriole length control.

Finally, centriole elongation could require another conserved family of proteins called POC1 (Keller et al., 2009). A role for POC1 proteins in centriole elongation is also supported by the study of two mutant lines defective for the *Drosophila* POC1 homologue. In these mutants, spermatid centrioles are shorter than in wild type, suggesting a partial impairment of centriole elongation (Blachon et al., 2009). In contrast, centrioles length is unaffected by POC1 depletion in *Tetrahymena* but basal bodies exhibit breaks in MT blades, suggesting that *Tetrahymena* POC1 may play a role in centriole stabilization rather than in length control (Pearson et al., 2009).

Besides elongation of MT triplets, centriole elongation involves the assembly of intra-luminal structures with the distal end of centrioles. Little is known about the function and molecular composition of these structures, which exhibit a remarkable degree of ultrastructural diversity among species. In mammalian cells, the distal lumen of centrioles is filled with a periodic stack of tilted discs (Ibrahim et al., 2009). In *Paramecium*, the lumen contains a helical structure (Dippell, 1968), whereas in *Tetrahymena* a cylindrical electron-dense structure is observed (Pearson et al., 2009). The lumen of *Chlamydomonas* basal bodies appears to be filled with fibers connecting the MT triplets to each other (Geimer and Melkonian, 2004). Despite this morphological variability, intraluminal structures in diverse eukaryotes seem to have common properties. In particular, the distal lumen of centrioles in mammalian cells, in ciliates and in *Chlamydomonas* all contain centrin proteins (Paoletti et al., 1996; Geimer and Melkonian, 2004; Ruiz et al., 2005; Stemm-Wolf et al., 2005). Centrin proteins are calcium-binding proteins related to calmodulin that associate with the centrioles of most species and are present in the genomes of all species that assemble motile cilia.

Vertebrate centrosomes contain only one mature centriole (the mother centriole) that bears two sets of symmetrical appendages, and only this mother centriole can attach to the plasma membrane and nucleate a primary cilium. A protein called Cep164 that

specifically localizes to the distal appendages has been identified in human cells but it is not known whether this protein is essential for distal appendages assembly. Formation of the distal appendages was recently shown to depend on Odf1 (Singla et al., 2010).

Centriole maturation is coupled to cell-cycle progression. In vertebrate cells, the full maturation of centrioles takes 1.5 cell cycles. A centriole formed during the previous cell cycle remains immature until mitosis, when the two sets of appendages are assembled at its distal end (Vorobjev and Chentsov Yu, 1982). In cells arrested in S phase for prolonged periods, the daughter centrioles never acquire the appendages, suggesting that the transition through G2 or mitosis is essential for centriole maturation (Guarguaglini et al., 2005).

In vertebrate cells, some proteins, including centrin and hPOC5, are seen to associate with daughter centrioles in increasing amounts as the cell cycle progresses. In addition, the centriolar pools of Centrin and hPOC5 are highly phosphorylated (Azimzadeh et al., 2009). Such modifications in centriole composition may be part of the maturation process.

1.2.6. *Bipolar spindle assembly*

The assembly of a microtubule-based bipolar spindle is a crucial step of chromosome segregation (reviewed in Duncan and Wakefield, 2011). In the conventional view of mitosis in animal somatic cell division centrosomes play a dominant role in MTs nucleation (reviewed in Varmark, 2004). However, higher plants and female meiotic cells of many animal species such as mouse, *Xenopus* and *Drosophila* although devoid of centrosomes assemble perfectly functional spindles (Calarco-Gillam et al., 1983; Heald et al., 1996; Matthies et al., 1996; Shimamura et al., 2004). Furthermore, cells that normally contain centrosomes such as *Drosophila* neuroblasts and ganglion mother cells can build functional anastral spindles that allow flies to develop to adulthood in the absence of functional centrosomes (Bonaccorsi et al., 2000; Megraw et al., 2001; Basto et al., 2006). Similarly, ablation of both

centrosomes during prophase in monkey CVG-2 cells by laser microsurgery, does not disrupt bipolar spindle assembly (Khodjakov et al., 2000). These results indicate that although when present centrosomes dominate, they are not essential for spindle assembly.

The ability of cells to build a spindle in the absence of centrosomes implies that redundant mechanisms must exist to generate and organize MTs. An alternative route to spindle formation in animal cells has been described most clearly in an *in vitro* system using *Xenopus* egg extracts. The addition of beads coated with mitotic chromatin to centrosome-free activated extracts initiates the formation of bipolar spindles possessing the same morphological features as those with centrosomes (Heald et al., 1996). This chromatin-directed MT assembly is thought to depend upon the small GTPase Ran (Carazo-Salas et al., 1999; Kalab et al., 1999; Moore et al., 2002; Kalab and Heald, 2008) and the guanine nucleotide exchange factor, RCC1 (Moore et al., 2002).

After nuclear envelope breakdown, RCC1 binds to condensing chromatin. This generates a gradient of Ran-GTP in the vicinity of the chromosomes. MT organization by Ran-GTP relies upon its liberation of cargo proteins from the nuclear import factor Importin- β (reviewed in Ciciarello et al., 2007). These liberated cargoes, termed spindle assembly factors, include TPX2, a spindle-associated protein required for targeting of the kinesin-like protein Kif15-A/XKlp2 to the MT minus ends (Wittmann et al., 2000; Gruss et al., 2001), and the MT-associated protein HURP (Wong and Fang, 2006). TPX2 induces aster formation via a physical interaction with Aurora A, contributing to the activation of this kinase (Trieselmann et al., 2003). Active Aurora A then stabilizes MTs via a protein complex containing Mps/XMAP215, Eg5 and HURP (Koffa et al., 2006). However, in the absence of pre-polymerised MTs, HURP has also been shown to act to stabilize MTs independently of this complex in a Ran-GTP-dependent manner (Casanova et al., 2008). Live imaging of MTs has conclusively demonstrated that in normal mitotic cells

kinetochores can initiate MT polymerisation independently of centrosomes. These kinetochore-driven MTs (kMTs) are incorporated into the growing spindle in a dynein-dependent process via their capture by astral MTs (reviewed in Rieder, 2005).

Another factor involved in spindle assembly is the chromosome passenger complex (CPC) - consisting of Aurora B, INCENP, Survivin and Borealin/Dasra-B - which is required for spindle bipolarity, chromosome alignment and cytokinesis. The CPC is present on chromosome arms during early prometaphase where it is involved in MT stabilization; at late prometaphase it re-localises to the inner centromeres where it regulates the stability of kinetochore-kMT interactions (reviewed in Ruchaud et al., 2007). However, the presence of the CPC along the spindle MTs and its requirement for central spindle formation and cytokinesis suggests that this complex plays a more general role in MT generation during spindle formation (Tseng et al., 2010). Several RNAi-based studies have shown that the *Drosophila* CPC complex is required for proper spindle formation and cytokinesis (Adams et al., 2001; Giet and Glover, 2001; Lange et al., 2002; Echard et al., 2004), and *Drosophila Incenp* mutants are characterized by a drastic delay in female meiotic spindle formation (Colombie et al., 2008). Interestingly, *Drosophila* spermatocytes possess a meiosis-specific form of Borealin, called Australin, that is required for chromosome alignment and segregation, central spindle formation, and cytokinesis (Gao et al., 2008).

Both fluorescence-speckled microscopy of anastral meiotic spindles in *Xenopus* and live imaging of the plus end-associated protein EB1 in cells without functional centrosomes have revealed that MT ends are distributed throughout the spindle (Burbank et al., 2006; Mahoney et al., 2006), suggesting that new MTs are generated at sites distant from centrosomes or chromatin during mitosis. Recent work has uncovered a set of 8 MAPs - that form a complex called Augmin in *Drosophila* and HAUS in mammals (homologous to Augmin subunits) - which appear to have a role in MT generation from within the spindle (Goshima et al., 2007;

Goshima et al., 2008; Hughes et al., 2008; Bucciarelli et al., 2009; Lawo et al., 2009; Uehara et al., 2009). These proteins are thought to recruit γ -tubulin to pre-existing spindle MTs thereby leading to MT nucleation within the spindle (Goshima et al., 2007; Goshima et al., 2008). In addition, Augmin has been shown to be essential for the formation of kinetochore-driven MTs in metaphase cells that re-assemble their spindles after cold-induced tubulin depolymerization (Bucciarelli et al., 2009).

While centrosomes, chromatin/kinetochores and probably pre-existing MTs are all sites of MT nucleation, there is evidence for additional sites at which new MTs can be nucleated. For example, the remnants of the nuclear envelope, membrane-based structures such as the Golgi apparatuses and the proposed spindle matrix are all candidates. Consistent with these views some Nucleoporin (Nup) proteins have been recently shown to associate with γ -tubulin (reviewed in Johansen et al., 2011). An example of membrane-driven MT nucleation is provided by *Drosophila* spermatocytes. *asp* mutant spermatocytes in which the centrosomes are displaced from their normal perinuclear position exhibit MT growth in the region of the nuclear envelope (Rebollo et al., 2004).

The cytoplasm (or undetectable cytoplasmic substructures), too, is able to generate MTs that contribute to spindle formation. Mouse oocyte cytoplasts nucleate asters of MTs that progressively interact with one another, forming bipolar spindles (Brunet et al., 1998). Recent work has shown that over 80 of such MTOCs exist in intact mouse oocytes undergoing meiosis (Schuh and Ellenberg, 2007). Acentrosomal MTOCs have also been observed in *Drosophila* cells devoid of centrosomes (Mottier-Pavie and Megraw, 2009) or devoid of centrosomes and incapable of chromatin-driven MT nucleation due to the presence of mutations in the *misato* gene (Mottier-Pavie et al., 2011). Together, these studies suggest that “cytoplasmic” MT nucleation during mitosis and meiosis is a widespread phenomenon.

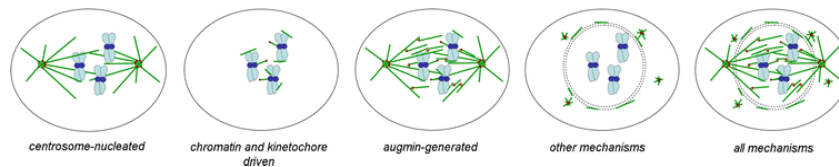


Figure 3. Mechanisms known to contribute to mitotic spindle formation. (from Duncan and Wakefield, 2011)

1.2.7. Spindle size

Although the spindle shows little size variation between cells of the same type, its length can vary dramatically both within and between species (reviewed in Goshima and Scholey, 2010). It has been proposed that spindle length is affected by both extrinsic and intrinsic factors. Well-known extrinsic factors are cell size and tubulin availability (Dumont and Mitchison, 2009; Goshima and Scholey, 2010). For example, during *Xenopus laevis* embryonic development cell size decreases from 1200 to 12 μm , and in cells smaller than 300 μm spindle length scales linearly with cell size (Wuhr et al., 2008). This suggests that constraints imposed by cell size and presumably tubulin availability set the spindle length. However, in the largest *X. laevis* blastomeres spindle length has an upper limit of 60 μm , implying the existence of intrinsic factors that govern spindle size (Wuhr et al., 2008). Further evidence for spindle size regulation by intrinsic factors is provided by the observation that spindles assembled in vitro from embryonic extracts of related *Xenopus* species display different species-specific sizes (Brown et al., 2007). Another example of spindle size regulation by intrinsic mechanisms is found in the 500 μm -long *Drosophila melanogaster* syncytial embryo, which displays 10 μm long spindles throughout the first 14 rounds of embryonic divisions (Sullivan and Theurkauf, 1995; Kwon and Scholey, 2004). Studies carried out in the past few years have identified several cell-size-independent intrinsic factors that regulate spindle length. These factors include proteins that mediate MT polymerization or depolymerization, MT sliding and MT clustering (Dumont and Mitchison, 2009; Goshima and

Scholey, 2010). However, perturbations of these factors result in relatively small changes in spindle length (Goshima and Scholey, 2010), suggesting that intrinsic factors are not sufficient to account for the large variations in spindle size observed in animal cells. While it is clear that spindle size depends on both intrinsic and extrinsic factors, the reasons for spindle size variability are largely unknown.

1.3 *Drosophila melanogaster* as model system to study cell division

The fruit fly *Drosophila melanogaster* has been widely used as a model organism because it offers several advantages. *Drosophila* requires only 10 days to progress from a fertilized egg to an adult; it is easy and cheap to maintain and to breed, and its genome is much smaller than the human genome. The *Drosophila* genome is organized in only four pairs of chromosomes, has been completely sequenced (Adams et al., 2000), and mutations or constructs for RNAi-driven gene inactivation are now available for most *Drosophila* genes. *D. melanogaster* is also an excellent model for studying cell division. Cells from different tissues are easily amenable for cytological analysis, including syncytial embryo nuclei, which are characterized by rapid and synchronized mitoses and repetitive assembly of multiple spindles within a common cytoplasm; neuroblasts, which are a particularly suitable model for the analysis of stem cell asymmetric division; male and female meiotic cells, as well several tissue culture cell lines. These different cells contain spindles that differ in architecture, thus providing an ideal material for studies aimed at the definition of common core mechanisms of spindle assembly (reviewed in Kwon and Scholey, 2004). Female meiotic cells are devoid of centrosomes and form “anastral” spindles using a chromosome-directed MT assembly pathway. Spindles in cultured S2 cells, embryos, neuroblasts and spermatocytes are “amphiastral” in that

they contain centrosomes and exhibit centrosome-driven asters at both spindle poles. However, when the centrosome-directed pathway fails, both S2 cells and larval neuroblasts efficiently use the chromatin-directed mechanisms of spindle formation. In addition, there is evidence that these cell types can form functional anastral spindles in the absence of centrosomes but are unable to form a functional spindle when chromatin-induced MT- generation is inhibited (Bucciarelli et al., 2009; Mottier-Pavie et al., 2011). In contrast, as detailed below, male meiotic spindle assembly requires MTs nucleated by the centrosomes but not chromatin-driven MTs (Bonaccorsi et al., 1998; Bucciarelli et al., 2003; Giansanti et al., 2008).

1.3.1. *Drosophila male meiosis*

Drosophila male meiosis offers several advantages for mutational and phenotypic analyses of cell division (Fuller, 1993; Cenci et al., 1994). Male meiosis occurs in the context of a complex developmental process, called spermatogenesis, that leads to the formation of 64 spermatozoa, starting from a single gonial cell generated by the asymmetric division of a germ line stem cell. A single founding gonial cell undergoes four rounds of mitotic divisions, all of which occur within an envelope formed by two somatic cyst cells. The 16 resultant postmitotic spermatocytes enter a 90-hour growth phase characterized by extensive transcription and translation accompanied by a 25-fold volume increase (reviewed in Fuller, 1993; Schafer et al., 1995; White-Cooper and Bausek, 2010).

Before completion of their growth phase, spermatocytes degrade the $\beta 1$ tubulin isotype and switch to the testis-specific $\beta 2$ isoform. Following this switch, all MT functions are carried out by a single tubulin heterodimer composed of the α -84B and β 2-tubulin isoforms (Kemphues et al., 1982; Hutchens et al., 1997). Meiosis I give rises to 32 secondary spermatocytes, which in turn rapidly undergo the second meiotic division, producing 64 spermatids. During both meiotic divisions, mitochondria line up along the

telophase central spindle and are equally partitioned between the two daughter cells. At the end of meiosis the mitochondria inherited by each cell fuse to form a complex structure called the Nebenkern. Thus, immediately following meiosis, at the so-called onion-stage, a single gonial cell-derived cyst is composed of 64 spermatids, each containing a single nucleus associated with a Nebenkern (Fig. 4). This peculiar structure of *Drosophila* spermatids provides one of the main advantages of male meiosis for genetic dissection of cell division, as meiotic mutants can be easily identified by spermatid examination. In wild type, each onion-stage spermatid consists of a round, phase-light nucleus associated with a single phase-dark Nebenkern of similar size. Defects in cell division result in nuclei and Nebenkern of different sizes and/or different nucleo:Nebenkern ratios (Fig. 4).

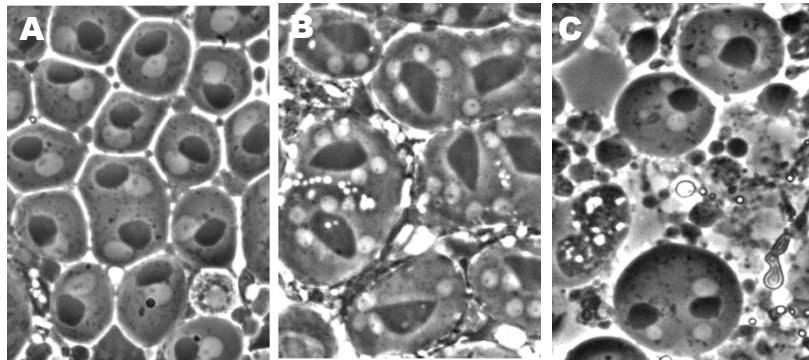


Figure 4. Onion stage spermatids from wild type (A) and mutant testes (B,C).

A further advantage of male meiosis is provided by the weak spindle checkpoint of spermatocytes (Rebollo and Gonzalez, 2000). This peculiar characteristic of male meiotic cells allows the analysis of late events in cell division such as central spindle assembly and cytokinesis in mutants affecting spindle assembly.

Finally, it should be noted that *D. melanogaster* spermatocytes form very large spindles that are well suited for cytological characterization of meiotic mutants (Fig. 5). The reason why

meiotic spindles of *Drosophila* males contain a peculiarly high number of MTs is addressed in the experimental part of this thesis.

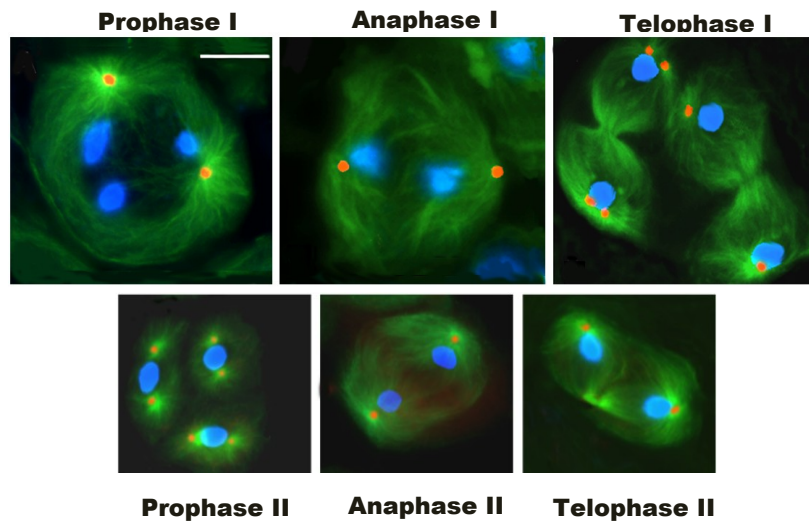


Figure 5. *Drosophila* male meiosis immunostained for tubulin (green) and the centrosomal protein centrosomin (red). DNA was stained with DAPI (blue).

Ramona Lattao

2. AIMS

The general aim of my PhD project was the analysis of *Drosophila* male meiosis, a model system that is becoming increasingly popular among students of cell divisions.

I first addressed a problem that has been puzzling people working on this system for many years: why is the fly male meiotic spindle so large as compared to the size of female meiotic spindle and the sizes of mitotic spindles of various cell types? I hypothesized that the size of male meiotic spindles reflects the availability of a large amount of tubulin synthesized premeiotically in spermatocytes to be used postmeiotically for the assembly of the long *Drosophila* sperm tail. To test this hypothesis, I examined male meiosis in 6 *Drosophila* species with dramatically different sperm flagella, ranging in length from 0.3 mm in *D. persimilis* to 58.3 mm in *D. bifurca* and found a perfect correlation between the spindle size and the sperm length.

My second aim was the identification and characterization of new genes that control male meiosis, focusing on those that affect the structure and/or the dynamic behaviour of meiotic centrosomes. Centrosomes are highly conserved structures and many centrosomal proteins identified in flies or *C. elegans* turned out to have human counterparts with roles in genetic diseases and/or carcinogenesis (see, for example Guernsey et al., 2010). Thus, identification of new *Drosophila* genes specifying centrosome-related functions may lead to the identification of new proteins implicated in human diseases. To facilitate the screen aimed at the identification of mutants affecting centrosome structure and behaviour I developed two novel balancer chromosomes that allow unambiguous recognition of mutant larvae from their heterozygous non-mutant siblings. Using these balancers, I screened a collection of male-sterile mutants for those that exhibit defects in spermatid

Ramona Lattao

morphology. I then performed a cytological characterization of meiosis of these mutants and identified two mutants with abnormal numbers of centrosomes: one mutant, I named *multi asters (most)* exhibits an excess of centrosomes, while the other mutant, *fragile centrioles (fract)*, has fewer centrosomes than wild type. I finely mapped then and cloned the genes specified by each of these mutants.

3. RESULTS AND DISCUSSION

3.1 Characterization of *Drosophila* male meiotic spindles

While male meiotic spindles and somatic cell spindles of mammals are comparable in size (Manandhar et al., 2000), spermatocyte spindles of *D. melanogaster* are much larger than those of mitotic cells (Cenci et al., 1994). In *D. melanogaster* primary spermatocytes, metaphase chromosomes appear as a small mass at the center of a large bipolar MT assembly. In contrast, in *D. melanogaster* embryonic cells, larval neuroblasts, ganglion mother cells and female meiotic cells, metaphase chromosomes occupy the entire equatorial region of the spindle or even protrude from the spindle (Theurkauf and Hawley, 1992; Sullivan and Theurkauf, 1995; Bonaccorsi et al., 2000; Kwon and Scholey, 2004). These differences in the basic shape of male meiotic spindles with respect to those in other fly cells are intriguing because there is no evidence that male meiotic spindles mediate chromosome segregation by any but normal mechanisms.

I hypothesized that *Drosophila* spermatocytes accumulate a substantial fraction of the tubulin needed for sperm tail assembly and use it for meiotic spindle formation. This hypothesis is testable, because various *Drosophila* species have dramatically different sperm flagella. *D. persimilis*, *D. Pseudoobscura*, *D. melanogaster*, *D. nanoptera* and *D. hydei* sperm tails are 0.32, 0.36, 1.91, 15.74 and 23.32 mm long, respectively; the *D. bifurca* flagellum is more than 30-fold longer than its *D. melanogaster* counterpart, with the extraordinary length of 58.29 mm (Pitnick et al., 1995a; Pitnick et al., 1995b). I examined male meiosis in these 6 *Drosophila* species to determine whether a correlation exists between sperm length and the size of the meiotic spindle.

To assess the spindle size, I measured both the length and the area of the spindle. The results of my analysis unequivocally

showed that the six *Drosophila* species differ dramatically in the length and the area of the spindles of the first meiotic division (Fig. 6A, B and C). Similar differences in size were observed in spindles of the second meiotic division (Fig. 6D and E). In all cases, I found a highly significant positive correlation between the spindle size of the meiotic figures and the length of the sperm flagellum (Fig. 6).

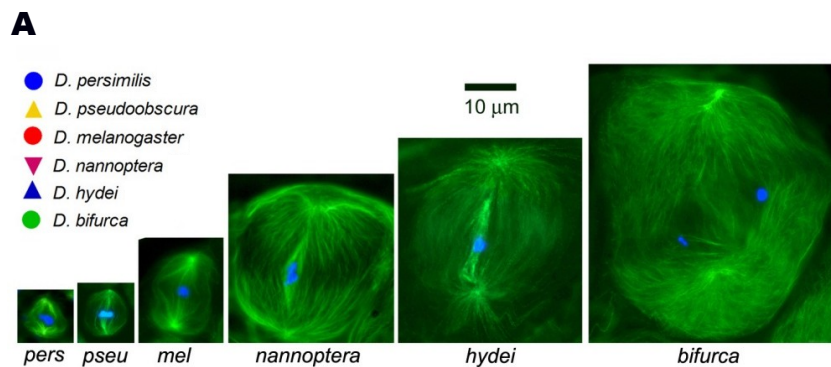


Figure 6. The size of the meiotic spindle from males of different *Drosophila* species positively correlates with the length of the sperm tail. **(A)** examples of meiotic metaphase I figures stained for tubulin (green). DNA was stained with DAPI (blue). Note that all spindles shown are at the same enlargement.

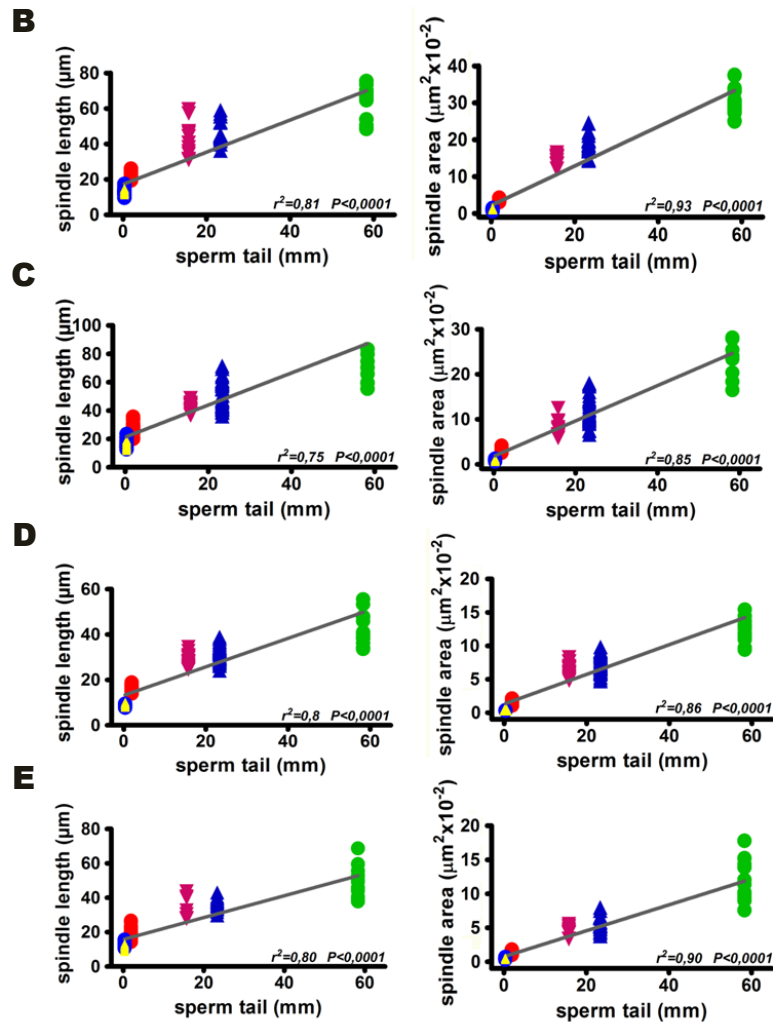


Figure 6bis. The graphs show the strong positive correlation between the length of the sperm tail and the spindle length or area in metaphase I (B), anatelophase I (C), metaphase II (D) and anatelophase II (E). The measures of the *D. persimilis* and *D. pseudoobscura* spindles are largely overlapping.

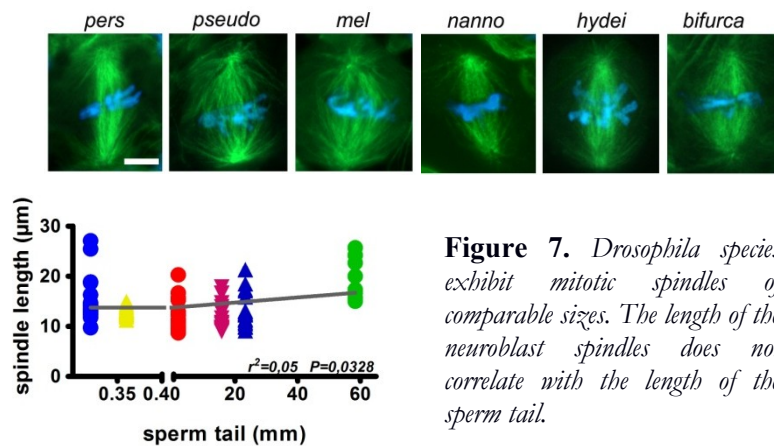
These observations support the hypothesis that primary spermatocytes of *Drosophila* species store amounts of tubulin that are proportional to the sperm tail length, and use a substantial part

of this tubulin to assemble the meiotic spindle. Consistent with this view, studies in mammalian cells have shown that approximately 50% of the available tubulin assembles into the mitotic spindle (Zhai and Borisy, 1994).

Several studies support the hypothesis that primary spermatocytes of *D. melanogaster* accumulate proteins required for spermiogenesis during the 90-hour growth phase (reviewed in Fuller, 1993; Schafer et al., 1995; White-Cooper and Bausek, 2010). Transcription is strongly reduced in postmeiotic cells of the *D. melanogaster* male germline and only a few genes appear to be transcriptionally active (Barreau et al., 2008; White-Cooper and Bausek, 2010). Spermatids inherit many stabilized mRNAs from spermatocytes including those that encode β 2-tubulin, and elongating spermatids undergo protein synthesis until late in spermiogenesis (reviewed in Fuller, 1993; White-Cooper, 2010). However, electron microscopy studies have shown that postmeiotic spermatids and mature sperm have a similar volume (Tokuyasu, 1975; Lindsley and Tokuyasu, 1980). This suggests that spermatocytes deliver to their meiotic products a substantial fraction of the material needed for sperm differentiation including the mitochondria and the tubulin. It should be noted that the delivery of tubulin and that of mitochondria are closely related events. During meiotic telophase I and II, mitochondria associate with the central spindle and are equally partitioned between the two daughter cells upon execution of cytokinesis (Fuller, 1993; Cenci et al., 1994). Thus, a spindle proportionate to sperm length ensures proper transmission to the spermatids of the two major components of the sperm tails: the tubulin and the mitochondria.

To control for the possibility that the differences in meiotic spindle size could be governed by species-specific factors other than the amount of tubulin needed to form the sperm tail, I examined mitotic division in larval brain squashes from all 6 *Drosophila* species. I observed that the spindle length in larval neuroblasts does not vary significantly between species, and that

the mitotic spindle size does not correlate with the sperm length (Fig. 7).



I also note that the large differences in meiotic spindles cannot be explained by obvious differences in chromosomal complements. Although these species exhibit different karyotypes, the number of chromosomes varies only between 8 and 12, and the diploid cells of all six species contain comparable amounts of DNA (Table1; Bosco et al., 2007). I thus conclude that there are no major species-specific factors that influence mitotic spindle size, making it unlikely that meiotic spindle size is regulated by factors other than the amount of tubulin accumulated in spermatocytes.

| Species | Fluorescence intensity (mean \pm SE) | DNA content (Mb) (mean \pm SE) | Previous DNA content estimates (Mb) | | |
|--------------------------------|--|----------------------------------|-------------------------------------|----------------------|------------|
| | | | Bosco et al., 2007 | | Others |
| | | | PI (mean \pm SE) | DAPI (mean \pm SE) | BC, CY, KI |
| <i>D. bifurca</i> (n=33) | 126 \pm 4 | 197 \pm 6 | - | - | - |
| <i>D. hydei</i> (n=24) | 144 \pm 5 | 226 \pm 8 | 164 \pm 16 | 177 \pm 22 | 197 -246 |
| <i>D. nanoptera</i> (n=39) | 138 \pm 3 | 217 \pm 5 | - | 236 \pm 35 | - |
| <i>D. melanogaster</i> (n=41) | 124 \pm 3 | 195 \pm 5 | 201 \pm 16 | 195 \pm 10 | 176-180 |
| <i>D. pseudoobscura</i> (n=14) | 146 \pm 6 | 230 \pm 10 | 185 \pm 12 | 135 \pm 6 | 168 |
| <i>D. persimilis</i> (n=29) | 143 \pm 4 | 226 \pm 6 | 183 \pm 10 | 170 \pm 34 | 197 |

Table 1. Bosco et al. have previously estimated the genome size (Mb) of 26 *Drosophila* species, including *D. persimilis*, *D. pseudoobscura*, *D. melanogaster*, *D. nanoptera* and *D. hydei* but not *D. bifurca*. To estimate the DNA content in the six *Drosophila* species studied here, I measured the fluorescence intensity of DAPI-stained brain cell nuclei using the Metamorph software. I selected the 30 % of nuclei showing the highest fluorescence intensities, assuming that these nuclei were in the late S-G2 phase of the cell cycle; the numbers between brackets indicate the number of selected nuclei. I then calculated the mean nuclear fluorescence intensity and the standard error (SE) for each species. Using as a standard the DNA content value (Mb) obtained by Bosco et al. for *D. melanogaster* using DAPI staining (195 Mb), I estimated the DNA content of all species including *D. bifurca*. "Previous estimates" refer to those of Bosco et al., obtained by flow cytometry of nuclei stained either by propidium iodide (PI) or DAPI, and to estimates obtained before Bosco's study (others). The latter values were obtained through biochemical analysis (BC), cytometry (CY), or kinetics (KI); references for these estimates can be found in Tab 3 of Bosco et al.

The metaphase spindle of *D. bifurca* primary spermatocytes with its 63 μ m of length is probably the largest spindle described to date in any organism (Goshima and Scholey, 2010). Very large are also the meiotic spindles of *D. hydei* and *D. nanoptera*. My results strongly suggest that the main extrinsic factor responsible for the large size of these spindles is tubulin availability.

However, the assembly of such large spindles requires a number of intrinsic factors. One of these factors could be the centriole/centrosome size. In *C. elegans* embryos, centriole/centrosome size correlates with spindle length (Greenan et al., 2010). Centriole and spindle lengths appear to be correlated as well in different *D. melanogaster* cell types; the centrioles of embryonic cells, tissue culture cells and spermatocytes are 0.2, 0.2 and 2.5 μ m long, respectively (Gonzalez et al., 1998; Baker et

al., 2004), while the metaphase spindle lengths in the same cells are 11.8, 10.0 and 23.0 μm , respectively (Goshima and Scholey, 2010). My cytological observations indicated that species with long sperm tails and large meiotic spindles also have large asters.

To assess the relationships between aster and spindle size, I measured the radius of the asters of late prophase/early prometaphase primary spermatocytes. I found that the aster radius positively correlates with the area of the metaphase spindle (Fig. 8), suggesting that the centrioles/centrosomes of large spindles indeed have a higher nucleating ability than those of small spindles. Consistent with this finding, EM studies have shown that the centrioles of *D. hydei* spermatocytes are approximately 3-fold longer than their *D. melanogaster* counterparts (Hennig and Kremer, 1990).

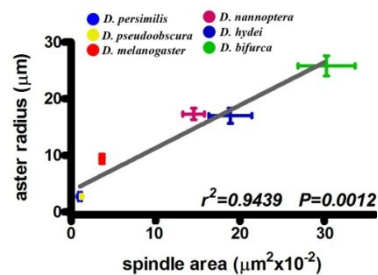


Figure 8. The size of the asters from males of different *Drosophila* species positively correlates with the spindle size. The graph shows the strong positive correlation between the radius of late prophase/early prometaphase asters and the area of metaphase spindles. The areas of metaphase spindles are the same as those in Figure 6. Error bars indicate standard deviations; the measures of the asters and spindles of *D. persimilis* and *D. pseudoobscura* are largely overlapping.

A positive correlation between the centrosome nucleating ability and the spindle size implies a major role of the centrosomes in meiotic spindle formation in males of *Drosophilidae*. A central role of centrosomal MTs in meiotic spindle assembly is supported by previous studies in *D. melanogaster*. In this species, centrosome-nucleated MTs are critical to spindle assembly in spermatocytes but not in somatic cells. Mutants in which centrosome function is inhibited form anastral but otherwise functional mitotic spindles by exploiting MTs nucleated near the

chromosomes (Bonaccorsi et al., 2000; Basto et al., 2006; Giansanti et al., 2008). However, although the same mutants nucleate MTs around the meiotic chromosomes, their male meiotic spindles are highly defective, leading to male sterility (Bonaccorsi et al., 1998; Giansanti et al., 2008). Consistent with these findings, *D. melanogaster* secondary spermatocytes have the peculiar ability to assemble a spindle in the complete absence of chromosomes, exploiting only MTs nucleated by the centrosomes (Bucciarelli et al., 2003). It is thus clear that centrosomal MTs have a preponderant role in meiotic spindle formation in *Drosophila* males, supporting the hypothesis that the centrosome is an important intrinsic factor in spindle size determination in *Drosophila* spermatocytes.

The reason why some *Drosophila* species evolved giant sperm tails is still matter of debate. The most popular current hypothesis asserts that the gametes and reproductive structures of males and females coevolved in response to sexual selection (Miller and Pitnick, 2002; Bjork and Pitnick, 2006; Joly and Schiffer, 2010).

My results underscore the strength of the selective forces that drove sperm length increase during *Drosophila* evolution.

Formation of the giant sperm tails was not simply achieved through an increase in postmeiotic translation of sperm proteins, but involved the evolution of giant spindles that utilize a substantial fraction of the tubulin that will be used after meiosis for sperm tail differentiation. The assembly of such spindles is likely to result from a series of concerted evolutionary changes in the regulation of spindle associated-proteins and in centrosome structure and function.

3.2 Generation of new *Tb*-marked balancer chromosomes

To identify new genes controlling centrosome structure and dynamics during *Drosophila* male meiosis I used a forward genetic approach. I screened a collection of stocks carrying male sterile or lethal mutations on chromosome II and III; these mutations were induced by EMS in Charles Zuker laboratory (University of California, San Diego) and kindly donated to us. The easiest way to maintain male sterile or lethal mutation is to keep them heterozygous over a multi-inverted balancer chromosome that suppresses recombination with its homologue.

One of the great advantages of *Drosophila melanogaster* as model organism is the availability of several balancer chromosomes. All balancers carry dominant markers that are visible in adult flies, but only a subset have markers that unambiguously distinguish homozygous mutant larvae from their heterozygous siblings. The latter balancers include those that express high levels of the GFP protein under the indirect control, via the UAS/GAL4 system, or there are direct-drive balancers that express GFP or YFP under the control of different promoters. Each of the GFP- or YFP-expressing balancers has specific advantages, but all share a common drawback: These balancers require the use of a dissecting microscope equipped with an UV light source, which for reliable fluorescence detection is preferably used in the dark. The *TM6B* balancer (Craymer, 1984) (chromosome III) carries the *Tb1* dominant mutation, which results in squat larvae and pupae. Drosophilists have been using this balancer for many years to unambiguously distinguish homozygous mitotic mutants dying at late larval stages from their heterozygous siblings (reviewed in Gatti and Baker, 1989). This balancer proved particularly useful when mutant larvae are rare and one has to examine several vials (or bottles) to find third instar larvae suitable for dissection and cytological analysis.

In my screen for new meiotic mutants, I used the *TM6B* balancer

for mutations mapping to the third chromosome. However, there was not a *Tb*-marked balancer for maintenance and analysis of mutations on the second chromosome. Thus, I decided to generate such a balancer together with a *Tb*-marked X chromosome balancer. To produce these balancers I inserted *Tb* dominant transgenes in the pre-existing of *FM7a* (Merriam, 1968) and *CyO* (Oster, 1956).

The Tubby phenotype results from the deletion in the *Tb1* chromosome of DNA encoding amino acids 167–190 of the *Twd1A* cuticle protein (Guan et al., 2006). Flies transformed with a genomic fragment spanning the *Twd1ATb1* transcription unit, as well as 1 kb of DNA upstream, exhibited the squat larval and pupal phenotype characteristic of the *Tb1* mutation. One such stock, referred to hereafter as *P{Tb1}/CyO*, was used as the starting point for mobilizing *Tb1* onto X and 2nd chromosome balancers. To generate *FM7a-P{Tb1}* I crossed *FM7a; P{Tb1}/CyO; TMS/+* males to *w/w* females (*TMS* is a $\Delta 2-3$ -bearing third chromosome balancer expressing the P-element transposase described in (Lindsley and Zimm, 1992); from approximately 1,000 progeny I recovered two *FM7* chromosomes that co-segregated with *Tb* (I propose to name these balancers *FM7-TbA* and *FM7-TbB*). To generate a second chromosome balancer with a *P{Tb1}* insertion I used a *CyO* balancer bearing the additional markers *S* and *bw¹*. I crossed *w/w; P{Tb1}/CyOSbw; TMS/+* females to *w; CyO/Sco* males and recovered three *CyO-Sbw-P{Tb1}* chromosomes from approximately 1,000 progeny (I propose to name these balancers *CyO-TbA*, *CyO-TbB* and *CyO-TbC*).

To assess the utility of these *FM7a* and *CyO Tb*-bearing balancers, I compared their *Tb* phenotype with the *Tb1* mutant phenotype associated with *TM6B* (Craymer, 1984). To quantify the squat phenotype elicited by the balancers I measured the axial ratio (Letsou et al., 1991) of larvae and pupae (AR, length/width) heterozygous for each balancer. It has been previously shown that the AR does not depend on larval and pupal size and provides a reliable measure of the *Tb* phenotype (Guan et al., 2006). As

shown in Figure 9, the ARs observed in *FM7-TbA*, *FM7-TbB*, *CyO-TbA*, *CyO-TbB*, *CyO-TbC* and *TM6B* heterozygotes are fully comparable and significantly different from those of wild type or non-*Tb*-bearing larvae and pupae. I thus conclude that the *FM7a* and *CyO* *Tb*-tagged chromosomes are highly suitable to distinguish larvae and pupae that bear the balancers from those that are homozygous for the balanced chromosome.

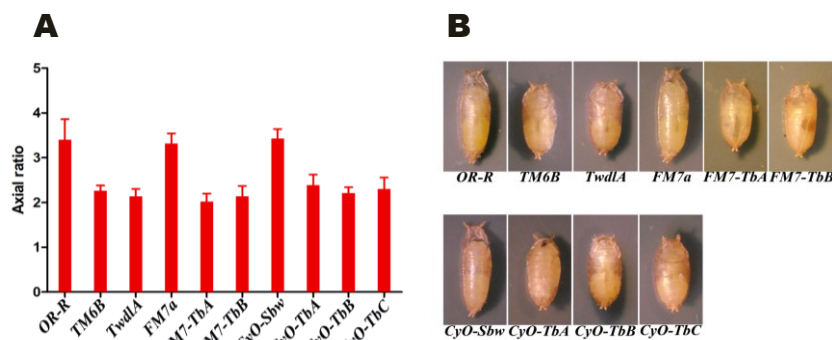


Figure 9. Quantitation of the squat phenotype of pupae heterozygous for different *Tb*-bearing chromosomes or balancers; OR-R is a wild type Oregon R stock; *TwdLA* contains a single copy of the *TwdLATb1* transgene; *FM7a* and *CyO-Sbw* are the balancer chromosomes used to construct the *Tb*-bearing derivatives indicated as *FM7-TbA*, *FM7-TbB*, *CyO-TbA*, *CyO-TbB* and *CyO-TbC*. **(A)** Axial ratios (ARs; length/width, \pm standard deviation) determined from digital photographs of at least 40 pupae of each genotype **(B)** examples of pupae heterozygous for different *Tb* mutations and transgenes.

Using inverse PCR I also determined the insertion sites of the *Tb1* transgenes within the *FM7-TbA* and *CyO-TbA* balancers. The insertion in *FM7-TbA* mapped at 17C in the intergenic space between *CG15047* and *beadex*; accordingly, this balancer is homozygous-viable. The *Tb1* transgene of *CyO-TbA* was inserted into the *Cytochrome P450 reductase (Cpr)* gene in region 26C3. In summary, I have generated *Tb*-marked versions of *FM7a* and *CyO*.

These chromosomes carry a stable *Tb1* transgene that has the same expressivity as the original *Tb1* mutation. The use of the *FM7-TbA* and *CyO-TbA* balancers will facilitate a number of

experimental strategies, allowing researchers to readily distinguish homozygous larvae and pupae from their heterozygous siblings simply by looking through the vial or the bottle used to grow the flies. In addition, the availability of balancers with different dominant larval markers such as *Tb* or GFP will allow construction of stocks carrying two lethal mutations balanced on *Tb*- and GFP-bearing balancers, respectively. This will be particularly helpful for selection and analysis of single and double mutants from the same culture.

3.3 Identification of *Drosophila* genes required for male meiosis by a cytological screen of male-sterile and lethal mutants

The third chromosome mutants of the “Zuker collection” were already balanced over *TM6B*. I took advantage of the *CyO-TbA* chromosome to rebalance the stocks carrying mutations on chromosome 2; these mutations were originally maintained over the *CyO* balancer, which lacks a larval marker.

As a first step of my screen (of 103 mutants), I identified the mutations that cause defects in spermatids morphology by in vivo analysis of squashed testes from homozygous mutant larvae selected for their non-Tubby phenotype. I then performed a cytological characterization of male meiosis of mutants with defective spermatids by immunostaining for tubulin and the centrosomal protein Centrosomin (Cnn, Li et al., 1998). These experiments led to the identification of two new genes that severely affect meiotic division: one on chromosome 3, I named *multi asters* (*most*); and one on chromosome 2, I named *fragile centrioles* (*fract*). The genetic and molecular characterization of these genes is reported below.

3.4 *Most*

3.4.1. *Cytological characterization of mutant phenotype*

*most*¹ is a male-sterile mutation that results in spermatids with nuclei of different sizes and abnormal Nebenkern/nucleus ratios. To identify the primary defect elicited by this mutation, I immunostained the testes from wild type controls and *most*¹ homozygous males with anti tubulin and anti-Cnn antibodies (Fig. 10). While wild type spermatocytes consistently showed bipolar spindles with a centrosome at each spindle pole, the large majority (>90%) of primary spermatocytes from *most*¹ mutants displayed multiple centrosomes associated with multipolar spindles and strong defects in chromosome segregation (in the rare anaphase-like figures). In addition, all meiotic cells failed to form a central spindle and undergo a regular telophase; they were therefore unable to undergo cytokinesis (Fig. 10).

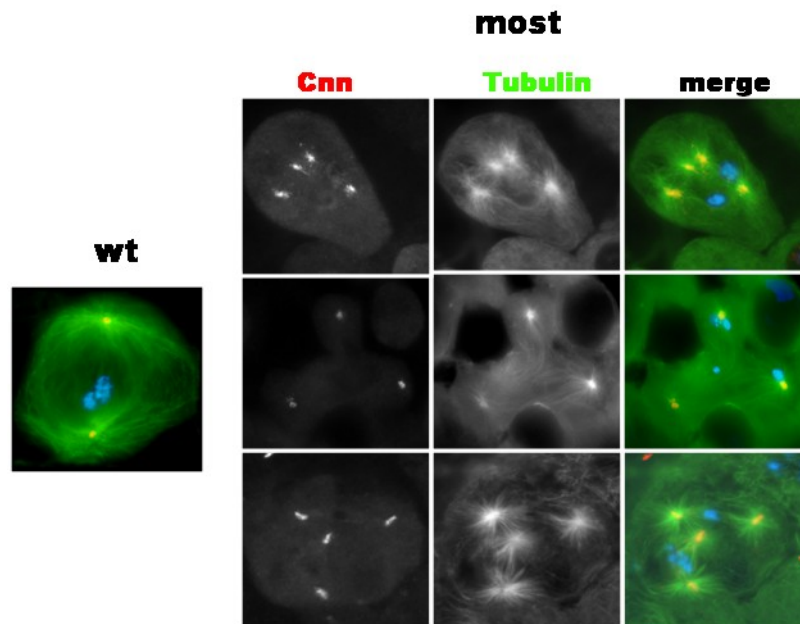


Figure 10. Male meiosis in wild type and *most*¹ homozygotes. Cells were stained for tubulin (green), Centrosomin (red). DNA was stained with DAPI (blue). Note the multipolar figures in mutant spermatocytes.

These observations suggest that dividing spermatocytes from *most* mutants are arrested in meiosis I. To substantiate this hypothesis, I immunostained control and mutant cells for Cyclin A (Fig. 11). In wild type spermatocytes, Cyclin A localizes to the cytoplasm in G2, enters the nucleus at the G2-M transition and then disappears. In *most*¹ mutants, Cyclin A never entered the nucleus and its cytoplasmic localization persisted even after nuclear envelope breakdown. These findings provide additional evidence that *most* mutant spermatocytes are unable to progress through meiosis.

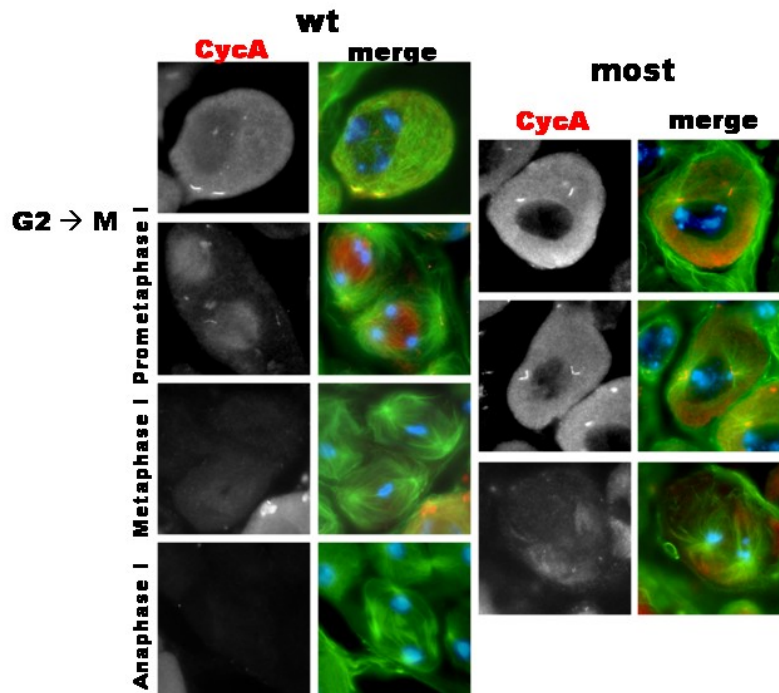


Figure 11. Male meiosis in wild type and *most*¹ homozygous males. Cells were immunostained for tubulin (green) and Cyclin A (red). DNA was stained with DAPI (blue). Note that that anti-Cyclin A antibody decorates the centrioles.

To further characterize the meiotic arrest phenotype of *most* mutants, I performed live imaging of meiotic cells expressing

tubulin-GFP (Fig. 12). Wild type prometaphase primary spermatocytes assembled a bipolar spindle in about 60 minutes ($n = 6$), in *most*^l mutant spermatocytes ($n = 5$) after 3 hours meiotic spindles were not yet fully assembled and cells only showed asters not connected by interpolar microtubules. I thus conclude that an impairment of the *most* function results in meiotic arrest in a prometaphase-like stage, with very few cells entering anaphase and none undergoing telophase.

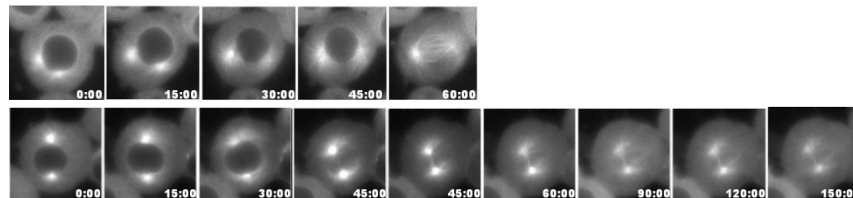


Figure 12. Time-lapse of male meiosis from prophase I to metaphase I in wild type (top row) and *most*^l (bottom row) testes.

3.4.2. Gene cloning

Recombination and deficiency mapping showed that *most*^l maps to the 76B1-B2 polytene chromosome region. DNA sequencing of the genes included this region revealed that *most* corresponds to *CG14087*, a gene of unknown function expressed only in primary spermatocytes (FlyBase, www.flybase.org). *most*^l mutants carry a deletion of 34bp (from bp 665 to 698) that results in a premature stop codon. This suggests that *most*^l is probably a null mutation.

To confirm the molecular identity of *most* I generated transgenic flies bearing *UAS-CG14087-GFP*. I then constructed *most*^l homozygous males carrying *UAS-CG14087-GFP* and the spermatocyte-specific *bam-GAL4* driver. These males did not show the spermatid phenotype of *most* mutants and were fertile. Thus, the expression of *CG14087* in spermatocytes completely rescues the meiotic defects elicited by *most* mutations (Fig. 13), showing that *most* is indeed *CG14087*.

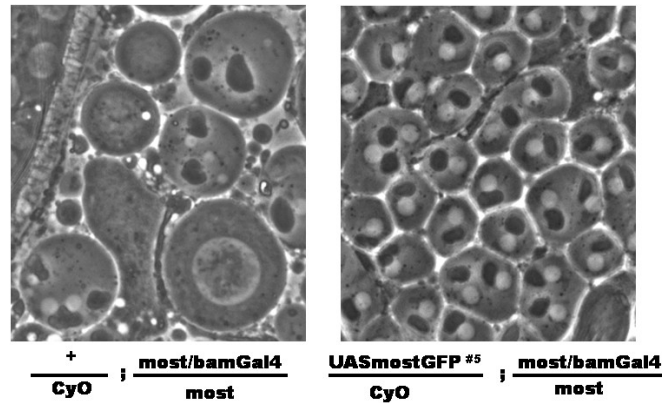


Figure 13. *Phenotype rescue in most¹ homozygotes in the presence of the UAS-CG14087-GFP transgene and the bamGAL4 driver.*

CG14087/most encodes a protein classified as a general transcription factor of the TFIID superfamily, with homology with the TBP-related factors. The testis-specific expression of Most might reflect a role of this protein in spermatocyte-specific gene transcription, which is coordinated by an alternative and specific form of RNA polymerase II transcription machinery (White-Cooper, 2010).

Previous studies have led to the identification of several genes collectively known as meiotic arrest genes (Lin et al., 1996). The meiotic arrest genes can be subdivided into the *always early* (*aly*) and *cannonball* (*can*) classes, based on their effects on spermatocyte cell cycle and spermatid differentiation. Mutants in the *aly*-class genes (including *aly*, *comr*, *achi/vis*, *topi* and *tomb*), fail to express the mRNA for the *twine* phosphatase, a Cdc25 homologue required for meiotic progression. Mutations in these genes also prevent the expression of a large set of genes required for spermatid differentiation. (White-Cooper et al., 1998; White-Cooper et al., 2000; Ayyar et al., 2003; Jiang and White-Cooper, 2003; Wang and Mann, 2003; Perezgasga et al., 2004; Beall et al., 2007; Jiang et al., 2007; Wang and Pan, 2007). Microarray analysis showed that at least 1000 genes are significantly underexpressed in the *aly*-class mutant testes compared to wild type. Homologues of

the *aly*-class meiotic arrest genes are evolutionarily conserved (Beitel et al., 2000; Korenjak et al., 2004) and have been shown to act as a complex to regulate gene expression in a cell cycle- and differentiation-dependent manner in several mammalian systems (Gagrica et al., 2004; Litovchick et al., 2007; Osterloh et al., 2007; Pilkinton et al., 2007).

The *can*-class genes (including *can*, *mia*, *nht*, *rye* and *sa*) encode testis-specific paralogues of the ubiquitously expressed TAF (TAFs) transcription factors. It has been proposed that the protein products of the *can*-class genes form different complexes to regulate the intricate gene expression program that characterizes *Drosophila* spermatogenesis (Hiller et al., 2004; Chen et al., 2005; Metcalf and Wassarman, 2007). Interestingly, while *can*-class mutants express the *twine* mRNA, they prevent the expression of an unknown factor required for *twine* mRNA translation (White-Cooper et al., 1998).

Testes of both *aly*- and *can*-class mutants only contain stages of spermatogenesis up to mature primary spermatocytes, which appear to arrest early in the G2-M transition of meiosis I. In these mutants, neither meiotic division nor spermatid differentiation occurs. The failure of spermatid differentiation is not a secondary defect of meiotic arrest, as *twine* mutant spermatocytes that omit meiosis eventually differentiate into spermatids. Thus, it has been suggested that the meiotic-arrest genes coordinate two independent pathways leading to meiotic division and spermatid differentiation (White-Cooper et al., 1993).

To identify the level at which *most* acts, I performed RT-PCR of mRNA from wild type and *most*^l testes, and found that *twine* is normally transcribed in *most* mutants (Fig. 14A). To determine whether *twine* mRNA is translated, I used flies expressing Twine-lacZ (kindly provided by H. White-Cooper; Cardiff University, UK (White-Cooper et al., 1998)). I constructed a stock expressing Twine-lacZ in a homozygous *most*^l mutant background. X-Gal staining revealed that in these testes there is no lacZ staining; in wild type testes X-Gal staining was positive indicating that *twine* is

translated (Fig. 14B). Collectively, these results indicate that Most acts at the level of *twine* translation, like the products of the *can*-class genes. However, the function of *most* differs from that of the *can*-class genes because mutations in *most* do not block spermatids differentiation (Fig. 15, and data not shown). It should be noted that Most is unlikely to be the unknown *can*-controlled factor required for *twine* translation, because *most* is regularly transcribed in *can* mutants. Thus, Most appears to control *twine* translation independently of the *can*-class genes.

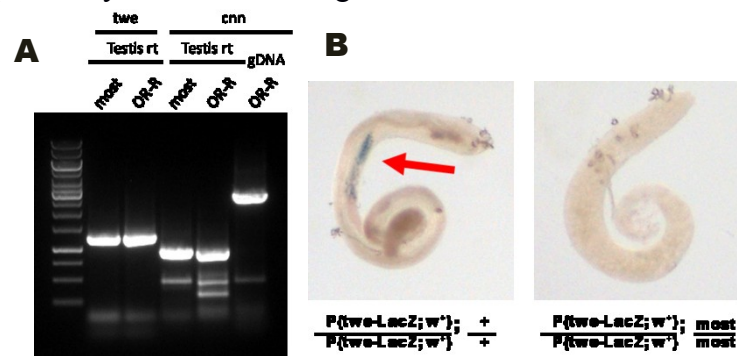


Figure 14. (A) RT-PCR of testis mRNA (*testis rt*) from wild type (OR-R) and *most*¹ flies. Because *most* has very small introns, to control for lack of contamination with unprocessed nuclear RNA, I performed RT-PCR of *cnn* mRNA and *cnn* genomic DNA (gDNA). (B) X-Gal staining of testes expressing the *twine-lacZ* reporter gene.

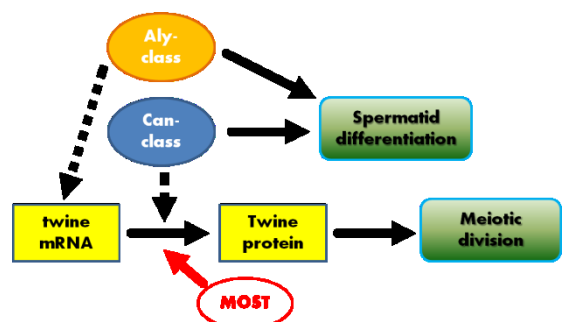


Figure 15. Diagram illustrating the possible role of Most in the molecular pathway that regulates *Drosophila* spermatogenesis.

3.5 *Fract*

3.5.1. *Cytological characterization of mutant phenotype*

Mutations in *fract*^l result in spermatids with micro- and macro-nuclei associated with abnormally-sized Nebenkern. Immunostaining for tubulin and Cnn revealed that 30% of meiosis II figures of *fract*^l mutants (n = 300) exhibit a bipolar monastral spindle with a single centrosome at the center of the aster. In these monastral secondary spermatocytes, chromosomes segregation was dramatically affected, giving rise to daughter nuclei with different DNA amounts (Fig. 16).

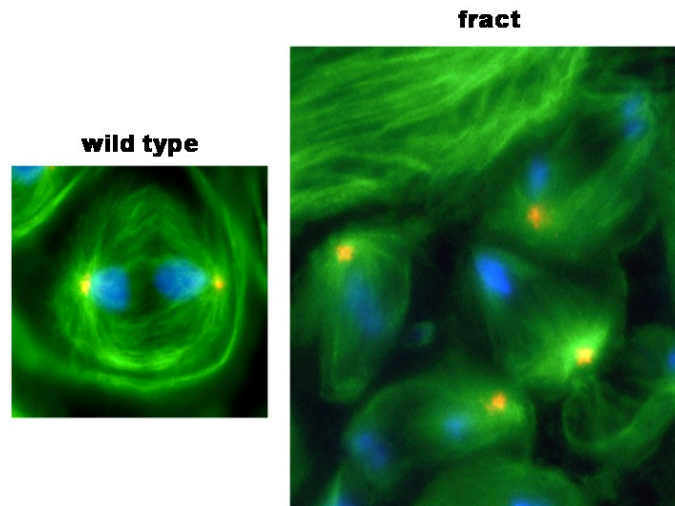


Figure 16. Meiosis II figures from wild type and *fract*^l homozygous males. Cells were immunostained for tubulin (green), and Cnn (red). DNA was stained with DAPI (blue). Note the bipolar monastral spindles in *fract* mutants.

To determine whether the meiotic phenotype of *fract*^l mutants was a consequence of defective centriole duplication or behavior, I immunostained wild type and mutant testes with an anti-Centrin1 antibody (Fig. 17; Paoletti et al., 1996). Wild type prophase I spermatocytes show two closely apposed pairs of centrioles, each arranged in the canonical V shape. In preparation of the first meiotic division these centriole pairs separate and progressively

migrate to the opposite cell poles. During late telophase I, the centrioles of each pair separate from each other to give rise to the secondary spermatocyte centrosomes, each containing a single centriole (Fig. 17 and data not shown).

In *fract*^l testes, all prophase spermatocytes (n = 50) showed two regular pairs of centrioles. However, ~ 10% (n = 50) of meiosis I figures displayed irregular centriole pairs. Most of these cells showed a normal centriole pair at one of the spindle poles, but at the other pole they had either a single centriole or a single intact centriole associated with a broken/degenerating centriole. Although the fraction of meiosis I cells with detectable defects in centrioles (10%) was lower than the fraction of monastral secondary spermatocytes (30%), these data strongly suggest that mutations in *fract* cause centriole loss during the first meiotic division and the short interphase that precedes the second.

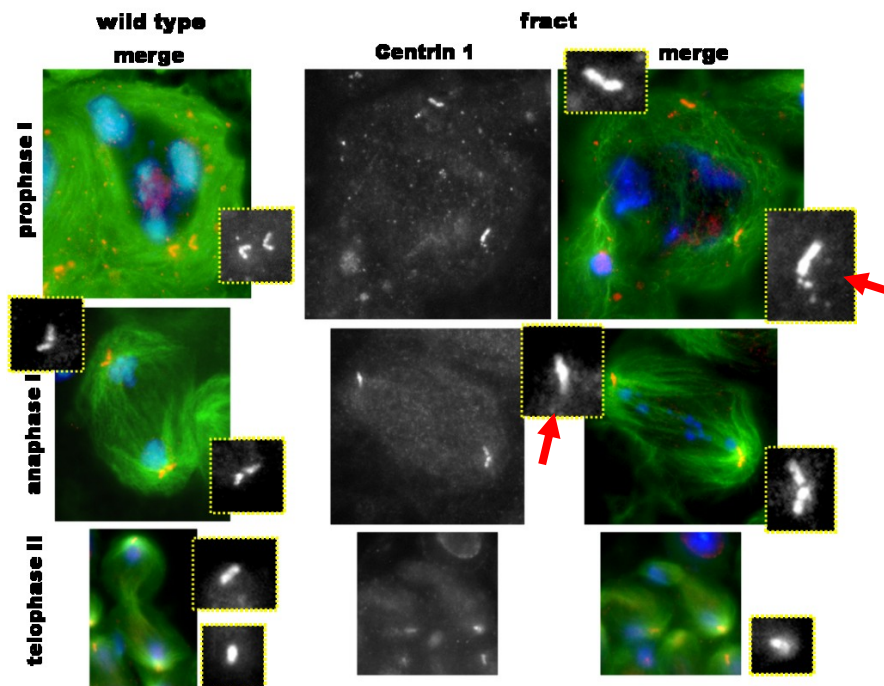


Figure 17. Wild type and *fract*¹ male meiotic figures immunostained for tubulin (green) and Centrin1 (red). DNA was stained with DAPI (blue). Note that in mutant primary spermatocytes one of the two centrioles is degenerating (arrows).

To further characterize the meiotic phenotype elicited by mutations in *fract*, I immunostained mutant testes with antibodies directed against two proteins (Asl, Sas4) involved in *Drosophila* centriole duplication. Both proteins showed a regular localization in prophase centrioles of *fract*¹ mutant spermatocytes. These findings reinforce the conclusion that Fract is required for maintenance of centriole integrity and not for centriole duplication.

3.5.2. Gene cloning

Recombination and deficiency mapping showed that *fract*¹ maps to the 46A1 polytene chromosome region. DNA sequencing of the genes included in this region revealed that *fract* corresponds to *CG10459*, a gene of unknown function expressed mainly in

testes. CG10459 encodes a protein of 322 aa that contains WD-repeats. Sequencing of the *fract^l* mutant allele revealed that it carries a base pair substitution that results in a premature stop codon, which leads to a truncated polypeptide of 295 aa. The *fract^l* mutation does not alter the mRNA stability, as shown by RT-PCR analysis (Fig. 18).

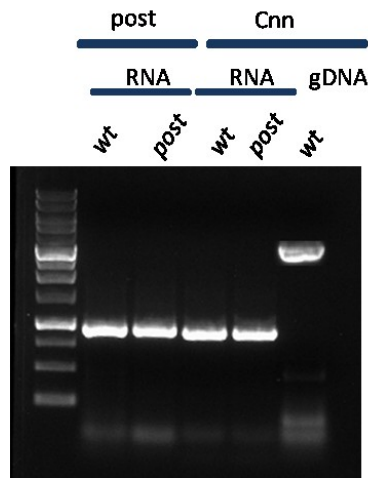


Figura 18. RT-PCR of *fract* mRNA from testes of wild type and *fract^l* males. To control for lack of contamination with unprocessed nuclear RNA, I performed RT-PCR of *cnn* mRNA and *cnn* genomic DNA (gDNA).

To confirm the molecular identity of *fract* I generated transgenic flies bearing *UAS-GFP-CG10459*. Expression of this transgene (using the *bam-GAL4* driver mentioned above) in testes of *fract^l* homozygotes partially rescued the meiotic phenotype elicited by the mutation, indicating that *fract* is indeed *CG10459*.

3.5.3. Subcellular localization of Fract

To obtain initial information on the subcellular localization of Fract I made a construct containing the UAS promoter, the *CG10459* coding region and the GFP coding sequence. This construct was cloned into the pPWG vector and co-transfected in *Drosophila* S2 cultured cells with a vector carrying Act-GAL4. Transfected cells expressed Fract-GFP, which formed aggregates that colocalized with the centrosomal marker γ -tubulin (Fig. 19).

This observation strongly suggests that Fract is a centrosomal component.

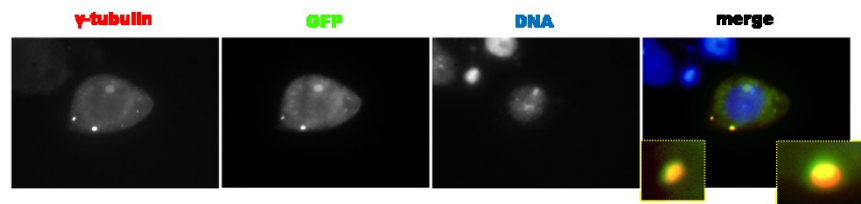


Figure 19. *S2 cells co-transfected with UAS-Fract-GFP and Act-Gal4 were immunostained for γ -tubulin and GFP. Dna was stained with DAPI. Note the co-localization of γ -tubulin and Fract-GFP.*

To confirm and further analyze the Fract subcellular localization, I decided to generate an anti-Fract antibody. I cloned the sequence encoding the Fract C-terminal 142 aa into the pET vector to obtain a 6XHis-tagged form of the polypeptide. I purified this polypeptide from *E.coli* and I used it to raise an antibody in chicken (see Materials and Methods). I obtained two anti-sera; one of them was affinity purified and used for Western blotting and immunostaining. In Western blots from wild type testis extracts, this antibody recognized a single band of the expected molecular weight (Fig. 20).

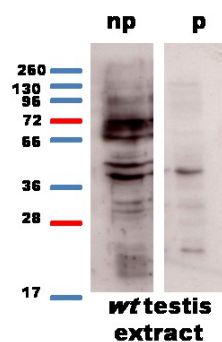


Figure 20. *Western blots of wild type testis extract stained with the non purified (np) or the affinity purified (p) anti-Fract antibody.*

I next immunostained fixed wild type testes with the anti-Fract antibody. I observed a highly specific staining pattern, with the

antibody decorating two dots at each spindle pole during meiosis I and one dot at each spindle pole during meiosis II (Fig. 21).

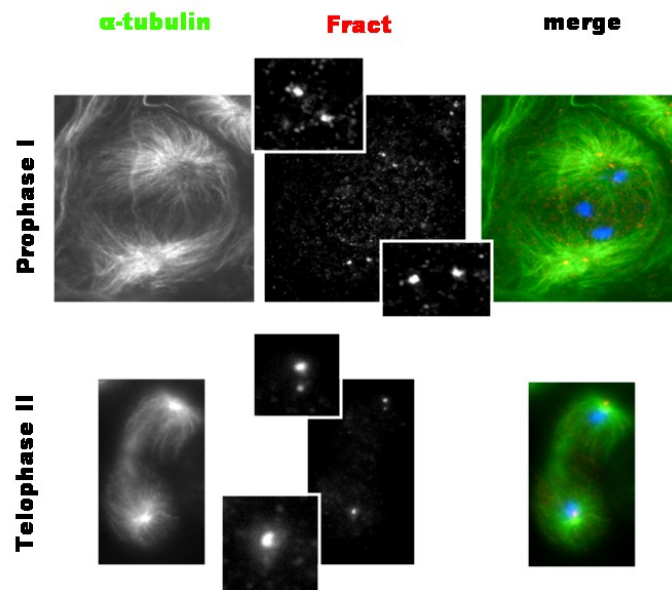


Figure 21. *Wild type male meiosis immunostained for tubulin (green) and Fract (red). DNA (blue) was stained with DAPI.*

To identify the structures immunostained by the anti-Fract antibody, I performed a co-localization analysis using antibodies directed against different centriolar/centrosomal components. Double immunostaining with the anti-Fract antibody and antibodies against γ -tubulin, DSpd-2 or Asl revealed that Fract specifically localizes at the distal ends of the centrioles and that the Fract signal partially overlaps the Asl signal (Fig. 22).

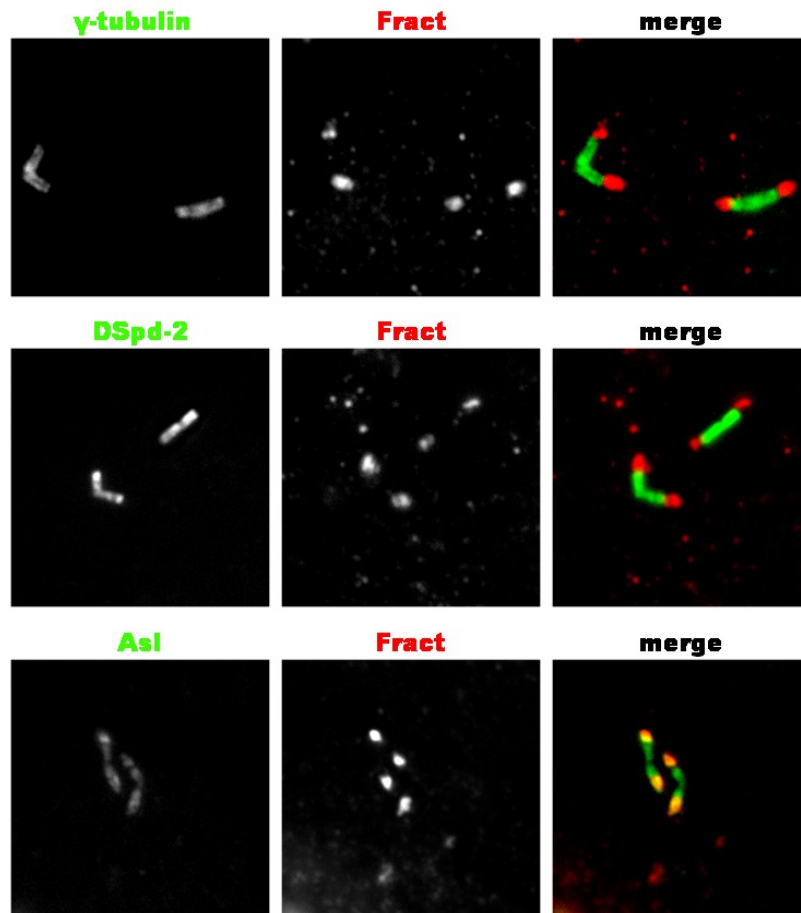


Figure 22. Double immunostainings of primary spermatocyte centrioles from wild type testes.

Transcript analysis by RT-PCR showed that *fract^l* mutants produce a stable mRNA (Fig. 18). Consistent with this result, Western blotting analysis performed on testis extracts from *fract^l* homozygous or hemizygous flies revealed that the mutant protein is still present in testes (Fig. 23).



Figure 23. Western blots of testis extracts from wild-type (OR-R), *fract*¹ homozygotes and *fract*¹ hemizygotes.

Surprisingly, immunostaining of *fract*¹ testes showed that the mutant protein is still associated with centrioles but not in the same way as in wild type; the truncated Fract protein is dispersed along the centrioles and is not specifically enriched only at their distal ends (Fig. 24A). This localization pattern was confirmed by double immunostaining of *fract*¹ mutant spermatocytes with the anti-Fract antibody and antibodies against γ -tubulin, DSpd-2 or Asl (Fig. 24B)

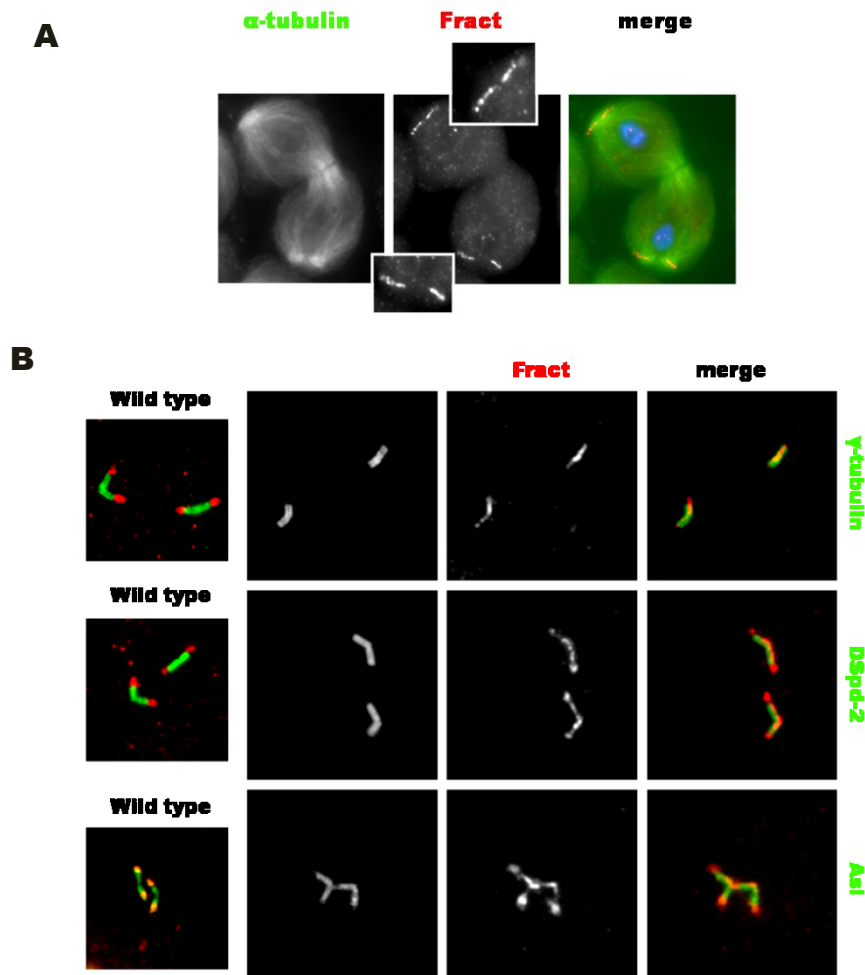


Figure 24. (A) Immunostaining for tubulin (green) and Fract (red) of a meiotic telophase I from *fract^l* mutant males. DNA (blue) was stained with DAPI. **(B)** Immunostaining of primary spermatocyte centrosomes with the anti-Fract antibody (red) and antibodies against γ -tubulin, DSpd-2 or Asl (green).

The localization pattern of the protein encoded by the *fract^l* mutant gene strongly suggests that the 27 aa C-terminal fragment of Fract is important for its specific enrichment at the distal ends of the centrosomes. A bioinformatic search for putative post-translational

modification sites on the C-terminal 27aa of Fract revealed a putative SUMOylation site on K310 (SUMOplot software). Because SUMOylation regulates different protein functions, including protein relocalization, it is tempting to speculate that proper Fract localization is mediated by SUMOylation.

3.5.4. Conclusions and perspectives

My results show that Fract is required to maintain centriole integrity during meiotic division of *Drosophila* males. The function specified by Fract is novel, as previous studies in a variety of organisms did not identify genes controlling centriole integrity. The observation that only one of the centrioles degenerates suggests that Fract is specifically required for the stability of either the mother or the daughter centriole. This hypothesis cannot be currently tested, due to the lack of antibodies or morphological features that allow unambiguous distinction between mother and daughter centrioles in *Drosophila* spermatocytes.

The finding that the Fract mutant protein is distributed along the entire centriole suggests two possible explanations for the observed mutant phenotype. The first is that Fract (or the truncated Fract encoded by *fract^l*) acts as a centriole-destabilizing factor that, when associated with the entire centriole, causes its fragmentation. The second explanation, which I favor, is that Fract is a “centriole capping” factor that must be concentrated at centriole ends to avoid centriole MT depolymerization.

There are several experiments I plan to do in the future. I would like to define the timing and the pattern of centriole degradation in *fract* mutants by *in vivo* analysis of *fract^l* mutant flies expressing the centriole marker YFP-Asl. In addition, I plan to generate (by RNAi or mutation) flies that do not express at all the Fract protein and analyze their male meiotic phenotype. Examination of these flies should answer the question of whether centriole degradation is caused by the spreading of the truncated Fract protein encoded by *fract^l*. Finally, to address the molecular mechanism of the Fract function, I will try to identify the Fract- interacting proteins by co-

immunoprecipitation using embryonic or larval extracts expressing Fract-GFP.

With another series of experiments I would like to define the mitotic phenotype of flies bearing mutations (or expressing an RNAi construct) that inactivate the *fract* paralogue wing morphogenesis defect (*wmd* or *CG3957*), which is expressed in the soma (FlyBase, www.flybase.org). The protein product of this gene is 31% identical and 33% similar to Fract (Ensembl, www.ensembl.org) and could very well be a component of somatic centrioles. The finding that Fract-GFP concentrates in centrosomes when ectopically expressed in S2 cells lends credibility to this possibility. If *wmd* turns out to play a role in mitotic centriole maintenance or function, in the long run I would like to address the role of its human counterpart (*STRAP*; 56% identity and 60% similarity, data from Ensembl, www.ensembl.org) by examining siRNA-treated tissue culture cells.

Ramona Lattao

4. MATERIALS AND METHODS

4.1 *Drosophila* strains

The *D. melanogaster* wild type stock used in this study is an Oregon R strain that has been kept in our laboratory for more than 30 years. The other species have been all obtained from the *Drosophila* Species Stock Center of the University of California, San Diego (<https://stockcenter.ucsd.edu>). *D. melanogaster*, *D. persimilis*, *D. pseudoobscura* and *D. hydei* were reared at 25°C on standard yeast-sucrose-agar medium. *D. nanoptera* and *D. bifurca* were grown on banana medium supplemented with opuntia cactus powder. The recipe for the banana/opuntia medium can be found at <https://stockcenter.ucsd.edu>.

4.2 Cytology

Larval neuroblast spindles were prepared according to Bonaccorsi et al. (Bonaccorsi et al., 2000). Meiotic spindle preparations were obtained from larval, pupal and adult testes, which were fixed and processed according to Cenci et al. (Cenci et al., 1994). Brain and testis preparations were incubated overnight at 4 °C with the following antibodies diluted in PBS: monoclonal anti tubulin antibody (1:1000; Sigma-Aldrich), rabbit anti-Cnn (1:1000, from T. Kaufman, Bloomington), rabbit anti-CycA (1:100, from C. Lehner, Bayreuth), rabbit Anti-Cen1 (1:300, from M. Bornens, Paris), rabbit anti-DSPd-2 (1:3500, from E. Bucciarelli, Rome), rabbit anti-GFP (1:1000; from G. Cestra, Rome) chicken anti-Fract (1:100). The primary antibodies were detected by 1 hour incubation at room temperature with FITC-conjugated anti-mouse IgG + IgM (1:15; Jackson Laboratories), Alexa555-conjugated anti-rabbit IgG (1:300; Molecular Probes) or anti-chicken (1:300; Jackson Laboratories), all diluted in PBS. Immunostained

preparations were mounted in Vectashield medium H-1200 (Vector Laboratories) containing the DNA dye DAPI (4,6 diamidino-2-phenylindole), and examined with a Zeiss Axioplan fluorescence microscope, equipped with a cooled charged-coupled device (CCD camera; Photometrics CoolSnap HQ). Grayscale digital images were collected separately, converted to Photoshop format, pseudocolored, and merged.

4.2.1. In vivo time lapse video microscopy

Testes isolated from third-instar larvae, pupae or adults were dissected under 10S volatile oil (Elf Atochem) onto a clean coverslip attached to the underside of an aluminium slide. Cells were examined with a Zeiss Axiovert 20 microscope equipped with an HBO 50W mercury lamp, and a filter wheel combination (Chroma Technology Corp.). The objectives used for spermatocytes were 63X (NA = 1.3). Images were acquired with a CoolSnap HQ camera (Photometrics). Image acquisition was controlled through a Metamorph software package (Universal imaging, Downing Town, PA). Images were collected at 1 min intervals; 10 (β -tubulin-EGFP) fluorescence optical sections were captured at 1 μ m z steps. Movies were created with the Metamorph software; each fluorescent image shown is the maximum-intensity projection of all the sections.

4.2.2. X-Gal Staining

X-Gal staining was performed according to White-Cooper et al., 1998. Testes were dissected in testis buffer (183 mM KCl, 47 mM NaCl, 10 mM Tris-HCl, pH 6.8) or in TB1 (15 mM potassium phosphate (equimolar dibasic and monobasic), pH 6.7, 80 mM KCl, 16 mM NaCl, 5 mM MgCl₂, 1% polyethylene glycol (PEG) 6000) and fixed in 4% formaldehyde in PBS for 15 min. The tissues were rinsed three times in X-gal buffer (150 mM NaCl, 7.2 mM Na₂HPO₄, 2.8 mM NaH₂PO₄, 1 mM MgCl₂) and left in this buffer for at least 30 min. Tissues were then incubated in staining solution (X-gal buffer containing 5 mM K₄Fe(CN)₆, 5 mM

K₃Fe(CN)₆) plus X-Gal at 37°C for 1 h to overnight, monitoring the reaction until color develops.

4.2.3. S2 cells transfection and staining

S2 cells were cultured at 25°C in Shields and Sang M3 medium (Sigma-Aldrich, St. Louis, MO) supplemented with 10% heat-inactivated fetal bovine serum (Sigma-Aldrich). To perform co-transfections, cells were suspended in serum-free Shields and Sang medium at a concentration of 1×10^6 cells/ml and plated, 1 ml/well in a six-well culture dish (Nalge Nunc, Naperville, IL). Each culture was inoculated with 1 µg plasmid supplemented with Cellfectin II (Life Technologies). After 5-h incubation at 25°C, 3 ml of medium supplemented with 10% fetal bovine serum was added to each culture. GFP expression was observed 48 h after transfection. Cells from 3-ml cultures were then harvested by centrifugation at $800 \times g$ for 5 min and washed in 10 ml of PBS. Pellet was resuspended in 3 ml of 4% paraformaldehyde in PBS and fixed for 15 min. Cells were then spun down by centrifugation, resuspended in 500 µl of PBS, and cytocentrifuged onto a clean slide using a cytocentrifuge (Shandon Scientific, Cheshire, England) at 900 rpm for 4 min. The slides were immersed in liquid nitrogen for at least 5 min, transferred to 0,05% SDS in PBS for 22 min, and then to 5% BSA in PBS for 22 min. These preparations were stained for tubulin and GFP using the specific antibodies described above.

4.2.4. Axial Ratio (A.R.) determination

For pupae, A.R. (length/width) was determined from digital photographs. At least 40 individuals were measured for each genotype.

4.2.5. Spindle and aster measurement

Spindle and aster measurements were carried out on digital images at defined enlargement. The spindle length is the distance between the two spindle poles. To calculate the spindle area we used the

MetaMorph program (Meta Imaging Series Software from Molecular Devices, Inc.).

4.2.6. Statistical analysis

Regression analysis was performed using the GraphPad software. The r^2 value measures the goodness-of-fit of linear regression; the P value evaluates the probability of the null hypothesis.

4.3 Molecular biology

4.3.1. Genomic DNA extraction

30 flies were homogenized in 500 μ l of 0,1 M TRIS-HCl pH9, 0,1 M EDTA, 1% SDS and left 30 min at 70°C. 112 μ l of K-Ac To were added the homogenate, which kept 30 min on ice. The sample was spun down at 12000 rpm for 15 min at 4°C, and after isopropanol addition, was centrifuged again. After a wash with 750 μ l of 70% ethanol, the sample was dried and resuspended in 60 μ l of H₂O. DNA was quantified using agarose gel 0,8% (TAE, agarose, EtBr).

4.3.2. RNA extraction and RT-PCR

50 males were dissected and testes are used for RNA extraction using RNeasy® Mini Kit (QIAGEN). For cDNA synthesis I employed SuperScript First-Strand Synthesis System for RT-PCR (Life Techonologies) using oligo dT primers.

4.3.3. Gene sequencing and cloning

For *Tb^I* cloning, a genomic fragment spanning the *TwdlATb^I* transcription unit, as well as 1 kb of DNA upstream, was inserted into a modified polylinker sequence in the pCaSpeR vector. Using standard methods, DNA was co-injected with a $\Delta 2-3$ transposase source into *w¹¹⁸* embryos; selected for *w+* eye color, and the transgene bearing chromosomes were maintained over balancers. For inverse PCR, genomic DNA was digested with EcoRI and the

fragment was ligated and amplified using the 5'-CAGCTCCATAGTTATAGCCGC and 5'-CGTTAAGTGGATGTCTTCTTG-3' primers.

For *CG14087* and *CG10459* sequencing, genomic DNA from wild type, *most*¹ and *fract*¹ flies was amplified by PCR using specific primers; the PCR products are sequenced from BMR Genomics (University of Padova). For *most* cloning, cDNA from wild type testes was amplified using 5'-CACCATGCCACGACCTTCG-3' and 5'-GTCTACTATTTCTTTTGG-3' primers; the PCR product was inserted into pENTR™/SD/D-TOPO vector (Life Technologies). An LR recombination reaction was then performed using Gateway LR Clonase™ II enzyme mix (Life Technologies) to transfer the *most* gene into pPWG vector (*Drosophila* Genome Resource Center, Bloomington). pPWG is a specialized vector for flies transformation; it contains P element sequences, a *white*⁺ marker for transformant selection, a UAS promoter, and a GFP N-terminal tag. pPWG-*most* vector was used for flies transformation that was carried out by Bestgene Inc (USA).

For *fract* cloning, cDNA from wild type testes was amplified using 5'-CACCATGAGGCATGAAATCG-3' and 5'-ACTGATGGATCCATTCTTCTCC-3' primers. The PCR product was inserted into a pENTR™/SD/D-TOPO vector and then in the pPWG vector as described above.

4.4 Biochemistry

4.4.1 Antibody induction and purification

A DNA sequence encoding a C-terminal portion of Fract (aa 181-322) was first cloned in the expression vector Champion™ pET200 of the Directional TOPO Expression Kit (Life Technologies). The expressed protein was affinity purified using Ni⁺ Sepharose™ 6 fast flow (GE Healthcare) and then used for chicken immunization according to standard protocols (GeneTel

laboratories LLC, USA). For antibody purification, the His-tagged Fract protein was blotted onto a PVDF membrane by standard electrophoretic transfer, visualized by Ponceau S staining, and the band of interest was cut out. Membrane was blocked with 3% BSA ("Pentax Fraction V") in TBS for 1 hour at room temp on a rocker, then washed 2 min in TBS. 2 ml serum diluted 5 times in TBS were allowed to bind the membrane overnight at 4°. After 2 washes with PBS, the antibody was eluted from the membrane with 1 ml of 0.2M glycine.

4.4.2. Western blot

Western blotting was performed according to standard protocols. The anti-Fract antibody was diluted 1:5000 (serum) or 1:100 (affinity purified antibody), and the anti-tubulin antibody (Sigma-Aldrich used as a loading control) was diluted 1:5000. Membranes were incubated overnight at 4°C. These primary antibodies were detected using HRP-conjugated anti-chicken (Jackson Laboratories) and anti-mouse (GE Healthcare) secondary antibody, and the ECL detection kit (GE Healthcare).

REFERENCES

- Adams, M. D., Celniker, S. E., Holt, R. A., Evans, C. A., Gocayne, J. D., Amanatides, P. G., Scherer, S. E., Li, P. W., Hoskins, R. A., Galle, R. F. et al.** (2000). The genome sequence of *Drosophila melanogaster*. *Science* **287**, 2185-2195.
- Adams, R. R., Maiato, H., Earnshaw, W. C. and Carmena, M.** (2001). Essential roles of *Drosophila* inner centromere protein (INCENP) and aurora B in histone H3 phosphorylation, metaphase chromosome alignment, kinetochore disjunction, and chromosome segregation. *J Cell Biol* **153**, 865-880.
- Alvey, P. L.** (1986). Do adult centrioles contain cartwheels and lie at right angles to each other? *Cell Biol Int Rep* **10**, 589-598.
- Andersen, J. S., Wilkinson, C. J., Mayor, T., Mortensen, P., Nigg, E. A. and Mann, M.** (2003). Proteomic characterization of the human centrosome by protein correlation profiling. *Nature* **426**, 570-574.
- Avidor-Reiss, T., Maer, A. M., Koundakjian, E., Polyanovsky, A., Keil, T., Subramaniam, S. and Zuker, C. S.** (2004). Decoding cilia function: defining specialized genes required for compartmentalized cilia biogenesis. *Cell* **117**, 527-539.
- Ayyar, S., Jiang, J., Collu, A., White-Cooper, H. and White, R. A.** (2003). *Drosophila* TGIF is essential for developmentally regulated transcription in spermatogenesis. *Development* **130**, 2841-2852.
- Azimzadeh, J., Hergert, P., Delougee, A., Euteneuer, U., Formstecher, E., Khodjakov, A. and Bornens, M.** (2009). hPOC5 is a centrin-binding protein required for assembly of full-length centrioles. *J Cell Biol* **185**, 101-114.
- Badano, J. L., Mitsuma, N., Beales, P. L. and Katsanis, N.** (2006). The ciliopathies: an emerging class of human genetic disorders. *Annu Rev Genomics Hum Genet* **7**, 125-148.
- Baker, J. D., Adhikarakunnathu, S. and Kernan, M. J.** (2004). Mechanosensory-defective, male-sterile unc mutants identify a

novel basal body protein required for ciliogenesis in *Drosophila*. *Development* **131**, 3411-3422.

Barnes, B. G. (1961). Ciliated secretory cells in the pars distalis of the mouse hypophysis. *J Ultrastruct Res* **5**, 453-467.

Barr, A. R. and Gergely, F. (2007). Aurora-A: the maker and breaker of spindle poles. *J Cell Sci* **120**, 2987-2996.

Barreau, C., Benson, E., Gudmannsdottir, E., Newton, F. and White-Cooper, H. (2008). Post-meiotic transcription in *Drosophila* testes. *Development* **135**, 1897-1902.

Basto, R., Lau, J., Vinogradova, T., Gardiol, A., Woods, C. G., Khodjakov, A. and Raff, J. W. (2006). Flies without centrioles. *Cell* **125**, 1375-1386.

Beall, E. L., Lewis, P. W., Bell, M., Rocha, M., Jones, D. L. and Botchan, M. R. (2007). Discovery of tMAC: a *Drosophila* testis-specific meiotic arrest complex paralogous to Myb-Muv B. *Genes Dev* **21**, 904-919.

Beitel, G. J., Lambie, E. J. and Horvitz, H. R. (2000). The *C. elegans* gene *lin-9*, which acts in an Rb-related pathway, is required for gonadal sheath cell development and encodes a novel protein. *Gene* **254**, 253-263.

Bettencourt-Dias, M., Rodrigues-Martins, A., Carpenter, L., Riparbelli, M., Lehmann, L., Gatt, M. K., Carmo, N., Balloux, F., Callaini, G. and Glover, D. M. (2005). SAK/PLK4 is required for centriole duplication and flagella development. *Curr Biol* **15**, 2199-2207.

Bjork, A. and Pitnick, S. (2006). Intensity of sexual selection along the anisogamy-isogamy continuum. *Nature* **441**, 742-745.

Blachon, S., Cai, X., Roberts, K. A., Yang, K., Polyanovsky, A., Church, A. and Avidor-Reiss, T. (2009). A proximal centriole-like structure is present in *Drosophila* spermatids and can serve as a model to study centriole duplication. *Genetics* **182**, 133-144.

Blachon, S., Gopalakrishnan, J., Omori, Y., Polyanovsky, A., Church, A., Nicastro, D., Malicki, J. and Avidor-Reiss, T. (2008). *Drosophila* asterless and vertebrate Cep152 Are orthologs essential for centriole duplication. *Genetics* **180**, 2081-2094.

- Blacque, O. E., Cevik, S. and Kaplan, O. I.** (2008). Intraflagellar transport: from molecular characterisation to mechanism. *Front Biosci* **13**, 2633-2652.
- Bonaccorsi, S., Giansanti, M. G. and Gatti, M.** (1998). Spindle self-organization and cytokinesis during male meiosis in asterless mutants of *Drosophila melanogaster*. *J Cell Biol* **142**, 751-761.
- Bonaccorsi, S., Giansanti, M. G. and Gatti, M.** (2000). Spindle assembly in *Drosophila* neuroblasts and ganglion mother cells. *Nat Cell Biol* **2**, 54-56.
- Bosco, G., Campbell, P., Leiva-Neto, J. T. and Markow, T. A.** (2007). Analysis of *Drosophila* species genome size and satellite DNA content reveals significant differences among strains as well as between species. *Genetics* **177**, 1277-1290.
- Boveri, T.** (1914). Zur Frage der Entstehung Maligner Tuoren. *Jena: Fisher Verlag*.
- Brittle, A. L. and Ohkura, H.** (2005). Centrosome maturation: Aurora lights the way to the poles. *Curr Biol* **15**, R880-882.
- Broadhead, R., Dawe, H. R., Farr, H., Griffiths, S., Hart, S. R., Portman, N., Shaw, M. K., Ginger, M. L., Gaskell, S. J., McKean, P. G. et al.** (2006). Flagellar motility is required for the viability of the bloodstream trypanosome. *Nature* **440**, 224-227.
- Brown, K. S., Blower, M. D., Maresca, T. J., Grammer, T. C., Harland, R. M. and Heald, R.** (2007). *Xenopus tropicalis* egg extracts provide insight into scaling of the mitotic spindle. *J Cell Biol* **176**, 765-770.
- Brunet, S., Polanski, Z., Verlhac, M. H., Kubiak, J. Z. and Maro, B.** (1998). Bipolar meiotic spindle formation without chromatin. *Curr Biol* **8**, 1231-1234.
- Bucciarelli, E., Giansanti, M. G., Bonaccorsi, S. and Gatti, M.** (2003). Spindle assembly and cytokinesis in the absence of chromosomes during *Drosophila* male meiosis. *J Cell Biol* **160**, 993-999.
- Bucciarelli, E., Pellacani, C., Naim, V., Palena, A., Gatti, M. and Somma, M. P.** (2009). *Drosophila* Dgt6 interacts with Ndc80,

Msp/XP202.1, and gamma-tubulin to promote kinetochore-driven MT formation. *Curr Biol* **19**, 1839-1845.

Burbank, K. S., Groen, A. C., Perlman, Z. E., Fisher, D. S. and Mitchison, T. J. (2006). A new method reveals microtubule minus ends throughout the meiotic spindle. *J Cell Biol* **175**, 369-375.

Calarco-Gillam, P. D., Siebert, M. C., Hubble, R., Mitchison, T. and Kirschner, M. (1983). Centrosome development in early mouse embryos as defined by an autoantibody against pericentriolar material. *Cell* **35**, 621-629.

Callaini, G., Whitfield, W. G. and Riparbelli, M. G. (1997). Centriole and centrosome dynamics during the embryonic cell cycles that follow the formation of the cellular blastoderm in *Drosophila*. *Exp Cell Res* **234**, 183-190.

Carazo-Salas, R. E., Guarguaglini, G., Gruss, O. J., Segref, A., Karsenti, E. and Mattaj, I. W. (1999). Generation of GTP-bound Ran by RCC1 is required for chromatin-induced mitotic spindle formation. *Nature* **400**, 178-181.

Casanova, C. M., Rybina, S., Yokoyama, H., Karsenti, E. and Mattaj, I. W. (2008). Hepatoma up-regulated protein is required for chromatin-induced microtubule assembly independently of TPX2. *Mol Biol Cell* **19**, 4900-4908.

Cavalier-Smith, T. (2002). The phagotrophic origin of eukaryotes and phylogenetic classification of Protozoa. *Int J Syst Evol Microbiol* **52**, 297-354.

Cenci, G., Bonaccorsi, S., Pisano, C., Verni, F. and Gatti, M. (1994). Chromatin and microtubule organization during premeiotic, meiotic and early postmeiotic stages of *Drosophila melanogaster* spermatogenesis. *J Cell Sci* **107** (Pt 12), 3521-3534.

Chen, X., Hiller, M., Sancak, Y. and Fuller, M. T. (2005). Tissue-specific TAFs counteract Polycomb to turn on terminal differentiation. *Science* **310**, 869-872.

Chen, Z., Indjeian, V. B., McManus, M., Wang, L. and Dynlacht, B. D. (2002). CP110, a cell cycle-dependent CDK substrate, regulates centrosome duplication in human cells. *Dev Cell* **3**, 339-350.

- Ciciarello, M., Mangiacasale, R. and Lavia, P.** (2007). Spatial control of mitosis by the GTPase Ran. *Cell Mol Life Sci* **64**, 1891-1914.
- Colombie, N., Cullen, C. F., Brittle, A. L., Jang, J. K., Earnshaw, W. C., Carmena, M., McKim, K. and Ohkura, H.** (2008). Dual roles of Incenp crucial to the assembly of the acentrosomal metaphase spindle in female meiosis. *Development* **135**, 3239-3246.
- Craymer, L.** (1984). TM6B: Third Multiple Six, B structure. *Dros Inf Serv* **60**, 234.
- Dammermann, A., Muller-Reichert, T., Pelletier, L., Habermann, B., Desai, A. and Oegema, K.** (2004). Centriole assembly requires both centriolar and pericentriolar material proteins. *Dev Cell* **7**, 815-829.
- Delattre, M. and Gonczy, P.** (2004). The arithmetic of centrosome biogenesis. *J Cell Sci* **117**, 1619-1630.
- Dictenberg, J. B., Zimmerman, W., Sparks, C. A., Young, A., Vidair, C., Zheng, Y., Carrington, W., Fay, F. S. and Doxsey, S. J.** (1998). Pericentrin and gamma-tubulin form a protein complex and are organized into a novel lattice at the centrosome. *J Cell Biol* **141**, 163-174.
- Dippell, R. V.** (1968). The development of basal bodies in paramecium. *Proc Natl Acad Sci U S A* **61**, 461-468.
- Dumont, S. and Mitchison, T. J.** (2009). Force and length in the mitotic spindle. *Curr Biol* **19**, R749-761.
- Duncan, T. and Wakefield, J. G.** (2011). 50 ways to build a spindle: the complexity of microtubule generation during mitosis. *Chromosome Res* **19**, 321-333.
- Echard, A., Hickson, G. R., Foley, E. and O'Farrell, P. H.** (2004). Terminal cytokinesis events uncovered after an RNAi screen. *Curr Biol* **14**, 1685-1693.
- Fuller, M.** (1993). Spermatogenesis. In *The Development of Drosophila melanogaster* (eds M Bate and A Martinez-Arias) (ed. N. Y. Cold Spring Harbor, NY), pp. 71-147.

- Gadde, S. and Heald, R.** (2004). Mechanisms and molecules of the mitotic spindle. *Curr Biol* **14**, R797-805.
- Gagrica, S., Hauser, S., Kolfshoten, I., Osterloh, L., Agami, R. and Gaubatz, S.** (2004). Inhibition of oncogenic transformation by mammalian Lin-9, a pRB-associated protein. *EMBO J* **23**, 4627-4638.
- Gao, S., Giansanti, M. G., Buttrick, G. J., Ramasubramanyan, S., Auton, A., Gatti, M. and Wakefield, J. G.** (2008). Australin: a chromosomal passenger protein required specifically for *Drosophila melanogaster* male meiosis. *J Cell Biol* **180**, 521-535.
- Gatti, M. and Baker, B. S.** (1989). Genes controlling essential cell-cycle functions in *Drosophila melanogaster*. *Genes Dev* **3**, 438-453.
- Geimer, S. and Melkonian, M.** (2004). The ultrastructure of the *Chlamydomonas reinhardtii* basal apparatus: identification of an early marker of radial asymmetry inherent in the basal body. *J Cell Sci* **117**, 2663-2674.
- Gerdes, J. M., Davis, E. E. and Katsanis, N.** (2009). The vertebrate primary cilium in development, homeostasis, and disease. *Cell* **137**, 32-45.
- Gherman, A., Davis, E. E. and Katsanis, N.** (2006). The ciliary proteome database: an integrated community resource for the genetic and functional dissection of cilia. *Nat Genet* **38**, 961-962.
- Giansanti, M. G., Bucciarelli, E., Bonaccorsi, S. and Gatti, M.** (2008). *Drosophila* SPD-2 is an essential centriole component required for PCM recruitment and astral-microtubule nucleation. *Curr Biol* **18**, 303-309.
- Gibbons, I. R.** (1981). Cilia and flagella of eukaryotes. *J Cell Biol* **91**, 107s-124s.
- Giet, R. and Glover, D. M.** (2001). *Drosophila* aurora B kinase is required for histone H3 phosphorylation and condensin recruitment during chromosome condensation and to organize the central spindle during cytokinesis. *J Cell Biol* **152**, 669-682.

- Glover, D. M.** (2005). Polo kinase and progression through M phase in *Drosophila*: a perspective from the spindle poles. *Oncogene* **24**, 230-237.
- Gomez-Ferreria, M. A., Rath, U., Buster, D. W., Chanda, S. K., Caldwell, J. S., Rines, D. R. and Sharp, D. J.** (2007). Human Cep192 is required for mitotic centrosome and spindle assembly. *Curr Biol* **17**, 1960-1966.
- Gonzalez, C., Tavosanis, G. and Mollinari, C.** (1998). Centrosomes and microtubule organisation during *Drosophila* development. *J Cell Sci* **111** (Pt 18), 2697-2706.
- Gopalakrishnan, J., Guichard, P., Smith, A. H., Schwarz, H., Agard, D. A., Marco, S. and Avidor-Reiss, T.** (2010). Self-assembling SAS-6 multimer is a core centriole building block. *J Biol Chem*.
- Goshima, G. and Scholey, J. M.** (2010). Control of mitotic spindle length. *Annu Rev Cell Dev Biol* **26**, 21-57.
- Goshima, G., Mayer, M., Zhang, N., Stuurman, N. and Vale, R. D.** (2008). Augmin: a protein complex required for centrosome-independent microtubule generation within the spindle. *J Cell Biol* **181**, 421-429.
- Goshima, G., Wollman, R., Goodwin, S. S., Zhang, N., Scholey, J. M., Vale, R. D. and Stuurman, N.** (2007). Genes required for mitotic spindle assembly in *Drosophila* S2 cells. *Science* **316**, 417-421.
- Greenan, G., Brangwynne, C. P., Jaensch, S., Gharakhani, J., Julicher, F. and Hyman, A. A.** (2010). Centrosome size sets mitotic spindle length in *Caenorhabditis elegans* embryos. *Curr Biol* **20**, 353-358.
- Gruss, O. J., Carazo-Salas, R. E., Schatz, C. A., Guarguaglini, G., Kast, J., Wilm, M., Le Bot, N., Vernos, I., Karsenti, E. and Mattaj, I. W.** (2001). Ran induces spindle assembly by reversing the inhibitory effect of importin alpha on TPX2 activity. *Cell* **104**, 83-93.
- Guan, X., Middlebrooks, B. W., Alexander, S. and Wasserman, S. A.** (2006). Mutation of TweedleD, a member of an

unconventional cuticle protein family, alters body shape in *Drosophila*. *Proc Natl Acad Sci U S A* **103**, 16794-16799.

Guarguaglini, G., Duncan, P. I., Stierhof, Y. D., Holmstrom, T., Duensing, S. and Nigg, E. A. (2005). The forkhead-associated domain protein Cep170 interacts with Polo-like kinase 1 and serves as a marker for mature centrioles. *Mol Biol Cell* **16**, 1095-1107.

Guernsey, D. L., Jiang, H., Hussin, J., Arnold, M., Bouyakdan, K., Perry, S., Babineau-Sturk, T., Beis, J., Dumas, N., Evans, S. C. et al. (2010). Mutations in centrosomal protein CEP152 in primary microcephaly families linked to MCPH4. *Am J Hum Genet* **87**, 40-51.

Guichard, P., Chretien, D., Marco, S. and Tassin, A. M. (2010). Procentriole assembly revealed by cryo-electron tomography. *EMBO J* **29**, 1565-1572.

Habedanck, R., Stierhof, Y. D., Wilkinson, C. J. and Nigg, E. A. (2005). The Polo kinase Plk4 functions in centriole duplication. *Nat Cell Biol* **7**, 1140-1146.

Heald, R., Tournebize, R., Blank, T., Sandaltzopoulos, R., Becker, P., Hyman, A. and Karsenti, E. (1996). Self-organization of microtubules into bipolar spindles around artificial chromosomes in *Xenopus* egg extracts. *Nature* **382**, 420-425.

Hennig, W. and Kremer, H. (1990). Spermatogenesis of *Drosophila hydei*. *Int Rev Cytol* **123**, 129-175.

Hildebrandt, F., Benzing, T. and Katsanis, N. (2011). Ciliopathies. *N Engl J Med* **364**, 1533-1543.

Hiller, M., Chen, X., Pringle, M. J., Suchorolski, M., Sancak, Y., Viswanathan, S., Bolival, B., Lin, T. Y., Marino, S. and Fuller, M. T. (2004). Testis-specific TAF homologs collaborate to control a tissue-specific transcription program. *Development* **131**, 5297-5308.

Hiraki, M., Nakazawa, Y., Kamiya, R. and Hirono, M. (2007). Bld10p constitutes the cartwheel-spoke tip and stabilizes the 9-fold symmetry of the centriole. *Curr Biol* **17**, 1778-1783.

Huangfu, D., Liu, A., Rakeman, A. S., Murcia, N. S., Niswander, L. and Anderson, K. V. (2003). Hedgehog signalling in the mouse requires intraflagellar transport proteins. *Nature* **426**, 83-87.

Hughes, J. R., Meireles, A. M., Fisher, K. H., Garcia, A., Antrobus, P. R., Wainman, A., Zitzmann, N., Deane, C., Ohkura, H. and Wakefield, J. G. (2008). A microtubule interactome: complexes with roles in cell cycle and mitosis. *PLoS Biol* **6**, e98.

Hung, L. Y., Tang, C. J. and Tang, T. K. (2000). Protein 4.1 R-135 interacts with a novel centrosomal protein (CPAP) which is associated with the gamma-tubulin complex. *Mol Cell Biol* **20**, 7813-7825.

Hutchens, J. A., Hoyle, H. D., Turner, F. R. and Raff, E. C. (1997). Structurally similar Drosophila alpha-tubulins are functionally distinct in vivo. *Mol Biol Cell* **8**, 481-500.

Ibrahim, R., Messaoudi, C., Chichon, F. J., Celati, C. and Marco, S. (2009). Electron tomography study of isolated human centrioles. *Microsc Res Tech* **72**, 42-48.

Jaspersen, S. L. and Winey, M. (2004). The budding yeast spindle pole body: structure, duplication, and function. *Annu Rev Cell Dev Biol* **20**, 1-28.

Jiang, J. and White-Cooper, H. (2003). Transcriptional activation in Drosophila spermatogenesis involves the mutually dependent function of aly and a novel meiotic arrest gene cookie monster. *Development* **130**, 563-573.

Jiang, J., Benson, E., Bausek, N., Doggett, K. and White-Cooper, H. (2007). Tombola, a tesmin/TSO1-family protein, regulates transcriptional activation in the Drosophila male germline and physically interacts with always early. *Development* **134**, 1549-1559.

Johansen, K. M., Forer, A., Yao, C., Girton, J. and Johansen, J. (2011). Do nuclear envelope and intranuclear proteins reorganize during mitosis to form an elastic, hydrogel-like spindle matrix? *Chromosome Res* **19**, 345-365.

- Joly, D. and Schiffer, M.** (2010). Coevolution of male and female reproductive structures in *Drosophila*. *Genetica* **138**, 105-118.
- Kalab, P. and Heald, R.** (2008). The RanGTP gradient - a GPS for the mitotic spindle. *J Cell Sci* **121**, 1577-1586.
- Kalab, P., Pu, R. T. and Dasso, M.** (1999). The ran GTPase regulates mitotic spindle assembly. *Curr Biol* **9**, 481-484.
- Keller, L. C., Romijn, E. P., Zamora, I., Yates, J. R., 3rd and Marshall, W. F.** (2005). Proteomic analysis of isolated chlamydomonas centrioles reveals orthologs of ciliary-disease genes. *Curr Biol* **15**, 1090-1098.
- Keller, L. C., Geimer, S., Romijn, E., Yates, J., 3rd, Zamora, I. and Marshall, W. F.** (2009). Molecular architecture of the centriole proteome: the conserved WD40 domain protein POC1 is required for centriole duplication and length control. *Mol Biol Cell* **20**, 1150-1166.
- Kemp, C. A., Kopish, K. R., Zipperlen, P., Ahringer, J. and O'Connell, K. F.** (2004). Centrosome maturation and duplication in *C. elegans* require the coiled-coil protein SPD-2. *Dev Cell* **6**, 511-523.
- Kemphues, K. J., Kaufman, T. C., Raff, R. A. and Raff, E. C.** (1982). The testis-specific beta-tubulin subunit in *Drosophila melanogaster* has multiple functions in spermatogenesis. *Cell* **31**, 655-670.
- Khodjakov, A. and Rieder, C. L.** (1999). The sudden recruitment of gamma-tubulin to the centrosome at the onset of mitosis and its dynamic exchange throughout the cell cycle, do not require microtubules. *J Cell Biol* **146**, 585-596.
- Khodjakov, A., Cole, R. W., Oakley, B. R. and Rieder, C. L.** (2000). Centrosome-independent mitotic spindle formation in vertebrates. *Curr Biol* **10**, 59-67.
- Kilburn, C. L., Pearson, C. G., Romijn, E. P., Meehl, J. B., Giddings, T. H., Jr., Culver, B. P., Yates, J. R., 3rd and Winey, M.** (2007). New Tetrahymena basal body protein components identify basal body domain structure. *J Cell Biol* **178**, 905-912.

- Kirkham, M., Muller-Reichert, T., Oegema, K., Grill, S. and Hyman, A. A.** (2003). SAS-4 is a *C. elegans* centriolar protein that controls centrosome size. *Cell* **112**, 575-587.
- Kleylein-Sohn, J., Westendorf, J., Le Clech, M., Habedanck, R., Stierhof, Y. D. and Nigg, E. A.** (2007). Plk4-induced centriole biogenesis in human cells. *Dev Cell* **13**, 190-202.
- Koffa, M. D., Casanova, C. M., Santarella, R., Kocher, T., Wilm, M. and Mattaj, I. W.** (2006). HURP is part of a Ran-dependent complex involved in spindle formation. *Curr Biol* **16**, 743-754.
- Kollman, J. M., Merdes, A., Mourey, L. and Agard, D. A.** (2011). Microtubule nucleation by gamma-tubulin complexes. *Nat Rev Mol Cell Biol* **12**, 709-721.
- Korenjak, M., Taylor-Harding, B., Binne, U. K., Satterlee, J. S., Stevaux, O., Aasland, R., White-Cooper, H., Dyson, N. and Brehm, A.** (2004). Native E2F/RBF complexes contain Myb-interacting proteins and repress transcription of developmentally controlled E2F target genes. *Cell* **119**, 181-193.
- Kumar, A., Girimaji, S. C., Duvvari, M. R. and Blanton, S. H.** (2009). Mutations in STIL, encoding a pericentriolar and centrosomal protein, cause primary microcephaly. *Am J Hum Genet* **84**, 286-290.
- Kuriyama, R. and Borisy, G. G.** (1981). Microtubule-nucleating activity of centrosomes in Chinese hamster ovary cells is independent of the centriole cycle but coupled to the mitotic cycle. *J Cell Biol* **91**, 822-826.
- Kwon, M. and Scholey, J. M.** (2004). Spindle mechanics and dynamics during mitosis in *Drosophila*. *Trends Cell Biol* **14**, 194-205.
- Lange, B. M., Rebollo, E., Herold, A. and Gonzalez, C.** (2002). Cdc37 is essential for chromosome segregation and cytokinesis in higher eukaryotes. *EMBO J* **21**, 5364-5374.
- Lawo, S., Bashkurov, M., Mullin, M., Ferreria, M. G., Kittler, R., Habermann, B., Tagliaferro, A., Poser, I., Hutchins, J. R., Hegemann, B. et al.** (2009). HAUS, the 8-subunit human Augmin

complex, regulates centrosome and spindle integrity. *Curr Biol* **19**, 816-826.

Leidel, S. and Gonczy, P. (2003). SAS-4 is essential for centrosome duplication in *C. elegans* and is recruited to daughter centrioles once per cell cycle. *Dev Cell* **4**, 431-439.

Leidel, S., Delattre, M., Cerutti, L., Baumer, K. and Gonczy, P. (2005). SAS-6 defines a protein family required for centrosome duplication in *C. elegans* and in human cells. *Nat Cell Biol* **7**, 115-125.

Letsou, A., Alexander, S., Orth, K. and Wasserman, S. A. (1991). Genetic and molecular characterization of tube, a *Drosophila* gene maternally required for embryonic dorsoventral polarity. *Proc Natl Acad Sci U S A* **88**, 810-814.

Li, K., Xu, E. Y., Cecil, J. K., Turner, F. R., Megraw, T. L. and Kaufman, T. C. (1998). *Drosophila* centrosomin protein is required for male meiosis and assembly of the flagellar axoneme. *J Cell Biol* **141**, 455-467.

Lin, T. Y., Viswanathan, S., Wood, C., Wilson, P. G., Wolf, N. and Fuller, M. T. (1996). Coordinate developmental control of the meiotic cell cycle and spermatid differentiation in *Drosophila* males. *Development* **122**, 1331-1341.

Lindsley, D. and Zimm. (1992). The Genome of *Drosophila melanogaster*.

Lindsley, D. L. and Tokuyasu, K. T. (1980). Spermatogenesis. In *The Genetics and Biology of Drosophila* (eds. M Ashburner and TRF Wright) (ed. S. D. Academic Press, CA.), pp. 225-294.

Litovchick, L., Sadasivam, S., Florens, L., Zhu, X., Swanson, S. K., Velmurugan, S., Chen, R., Washburn, M. P., Liu, X. S. and DeCaprio, J. A. (2007). Evolutionarily conserved multisubunit RBL2/p130 and E2F4 protein complex represses human cell cycle-dependent genes in quiescence. *Mol Cell* **26**, 539-551.

Loncarek, J., Hergert, P., Magidson, V. and Khodjakov, A. (2008). Control of daughter centriole formation by the pericentriolar material. *Nat Cell Biol* **10**, 322-328.

- Luders, J. and Stearns, T.** (2007). Microtubule-organizing centres: a re-evaluation. *Nat Rev Mol Cell Biol* **8**, 161-167.
- Mahoney, N. M., Goshima, G., Douglass, A. D. and Vale, R. D.** (2006). Making microtubules and mitotic spindles in cells without functional centrosomes. *Curr Biol* **16**, 564-569.
- Manandhar, G., Moreno, R. D., Simerly, C., Toshimori, K. and Schatten, G.** (2000). Contractile apparatus of the normal and abortive cytokinetic cells during mouse male meiosis. *J Cell Sci* **113 Pt 23**, 4275-4286.
- Matthies, H. J., McDonald, H. B., Goldstein, L. S. and Theurkauf, W. E.** (1996). Anastral meiotic spindle morphogenesis: role of the non-claret disjunctional kinesin-like protein. *J Cell Biol* **134**, 455-464.
- Megraw, T. L., Kao, L. R. and Kaufman, T. C.** (2001). Zygotic development without functional mitotic centrosomes. *Curr Biol* **11**, 116-120.
- Merriam, J.** (1968). FM7: First multiple seven. *Dros Inf Serv* **43**, 64.
- Metcalf, C. E. and Wassarman, D. A.** (2007). Nucleolar colocalization of TAF1 and testis-specific TAFs during Drosophila spermatogenesis. *Dev Dyn* **236**, 2836-2843.
- Mikule, K., Delaval, B., Kaldis, P., Jurczyk, A., Hergert, P. and Doxsey, S.** (2007). Loss of centrosome integrity induces p38-p53-p21-dependent G1-S arrest. *Nat Cell Biol* **9**, 160-170.
- Miller, G. T. and Pitnick, S.** (2002). Sperm-female coevolution in Drosophila. *Science* **298**, 1230-1233.
- Moore, W., Zhang, C. and Clarke, P. R.** (2002). Targeting of RCC1 to chromosomes is required for proper mitotic spindle assembly in human cells. *Curr Biol* **12**, 1442-1447.
- Moritz, M., Zheng, Y., Alberts, B. M. and Oegema, K.** (1998). Recruitment of the gamma-tubulin ring complex to Drosophila salt-stripped centrosome scaffolds. *J Cell Biol* **142**, 775-786.
- Mottier-Pavie, V. and Megraw, T. L.** (2009). Drosophila bld10 is a centriolar protein that regulates centriole, basal body, and motile cilium assembly. *Mol Biol Cell* **20**, 2605-2614.

- Mottier-Pavie, V., Cenci, G., Verni, F., Gatti, M. and Bonaccorsi, S.** (2011). Phenotypic analysis of misato function reveals roles of noncentrosomal microtubules in *Drosophila* spindle formation. *J Cell Sci* **124**, 706-717.
- Nakazawa, Y., Hiraki, M., Kamiya, R. and Hirono, M.** (2007). SAS-6 is a cartwheel protein that establishes the 9-fold symmetry of the centriole. *Curr Biol* **17**, 2169-2174.
- Nigg, E. A.** (2007). Centrosome duplication: of rules and licenses. *Trends Cell Biol* **17**, 215-221.
- Nigg, E. A. and Raff, J. W.** (2009). Centrioles, centrosomes, and cilia in health and disease. *Cell* **139**, 663-678.
- Nonaka, S., Tanaka, Y., Okada, Y., Takeda, S., Harada, A., Kanai, Y., Kido, M. and Hirokawa, N.** (1998). Randomization of left-right asymmetry due to loss of nodal cilia generating leftward flow of extraembryonic fluid in mice lacking KIF3B motor protein. *Cell* **95**, 829-837.
- O'Connell, C. B. and Khodjakov, A. L.** (2007). Cooperative mechanisms of mitotic spindle formation. *J Cell Sci* **120**, 1717-1722.
- O'Connell, K. F., Caron, C., Kopish, K. R., Hurd, D. D., Kemphues, K. J., Li, Y. and White, J. G.** (2001). The *C. elegans* zyg-1 gene encodes a regulator of centrosome duplication with distinct maternal and paternal roles in the embryo. *Cell* **105**, 547-558.
- Oakley, C. E. and Oakley, B. R.** (1989). Identification of gamma-tubulin, a new member of the tubulin superfamily encoded by mipA gene of *Aspergillus nidulans*. *Nature* **338**, 662-664.
- Oegema, K., Wiese, C., Martin, O. C., Milligan, R. A., Iwamatsu, A., Mitchison, T. J. and Zheng, Y.** (1999). Characterization of two related *Drosophila* gamma-tubulin complexes that differ in their ability to nucleate microtubules. *J Cell Biol* **144**, 721-733.
- Ohta, T., Essner, R., Ryu, J. H., Palazzo, R. E., Uetake, Y. and Kuriyama, R.** (2002). Characterization of Cep135, a novel coiled-

coil centrosomal protein involved in microtubule organization in mammalian cells. *J Cell Biol* **156**, 87-99.

Oster, I. (1956). A new crossing-over suppressor in chromosome 2 effective in the presence of heterologous inversions. *Dros Inf Serv* **56**.

Osterloh, L., von Eyss, B., Schmit, F., Rein, L., Hubner, D., Samans, B., Hauser, S. and Gaubatz, S. (2007). The human synMuv-like protein LIN-9 is required for transcription of G2/M genes and for entry into mitosis. *EMBO J* **26**, 144-157.

Ostrowski, L. E., Blackburn, K., Radde, K. M., Moyer, M. B., Schlatzer, D. M., Moseley, A. and Boucher, R. C. (2002). A proteomic analysis of human cilia: identification of novel components. *Mol Cell Proteomics* **1**, 451-465.

Paoletti, A., Moudjou, M., Paintrand, M., Salisbury, J. L. and Bornens, M. (1996). Most of centrin in animal cells is not centrosome-associated and centrosomal centrin is confined to the distal lumen of centrioles. *J Cell Sci* **109 (Pt 13)**, 3089-3102.

Pazour, G. J. (2004). Comparative genomics: prediction of the ciliary and basal body proteome. *Curr Biol* **14**, R575-577.

Pazour, G. J., Agrin, N., Leszyk, J. and Witman, G. B. (2005). Proteomic analysis of a eukaryotic cilium. *J Cell Biol* **170**, 103-113.

Pearson, C. G., Osborn, D. P., Giddings, T. H., Jr., Beales, P. L. and Winey, M. (2009). Basal body stability and ciliogenesis requires the conserved component Poc1. *J Cell Biol* **187**, 905-920.

Pelletier, L., O'Toole, E., Schwager, A., Hyman, A. A. and Muller-Reichert, T. (2006). Centriole assembly in *Caenorhabditis elegans*. *Nature* **444**, 619-623.

Pelletier, L., Ozlu, N., Hannak, E., Cowan, C., Habermann, B., Ruer, M., Muller-Reichert, T. and Hyman, A. A. (2004). The *Caenorhabditis elegans* centrosomal protein SPD-2 is required for both pericentriolar material recruitment and centriole duplication. *Curr Biol* **14**, 863-873.

Perezgasga, L., Jiang, J., Bolival, B., Jr., Hiller, M., Benson, E., Fuller, M. T. and White-Cooper, H. (2004). Regulation of

transcription of meiotic cell cycle and terminal differentiation genes by the testis-specific Zn-finger protein matotopetli. *Development* **131**, 1691-1702.

Pfaff, K. L., Straub, C. T., Chiang, K., Bear, D. M., Zhou, Y. and Zon, L. I. (2007). The zebra fish cassiopeia mutant reveals that SIL is required for mitotic spindle organization. *Mol Cell Biol* **27**, 5887-5897.

Piehl, M., Tulu, U. S., Wadsworth, P. and Cassimeris, L. (2004). Centrosome maturation: measurement of microtubule nucleation throughout the cell cycle by using GFP-tagged EB1. *Proc Natl Acad Sci U S A* **101**, 1584-1588.

Pilkinton, M., Sandoval, R. and Colamonici, O. R. (2007). Mammalian Mip/LIN-9 interacts with either the p107, p130/E2F4 repressor complex or B-Myb in a cell cycle-phase-dependent context distinct from the Drosophila dREAM complex. *Oncogene* **26**, 7535-7543.

Pitnick, S., Markow, T. A. and Spicer, G. S. (1995a). Delayed male maturity is a cost of producing large sperm in Drosophila. *Proc Natl Acad Sci U S A* **92**, 10614-10618.

Pitnick, S., Spicer, G. S. and Markow, T. A. (1995b). How long is a giant sperm? *Nature* **375**, 109.

Raff, J. W., Kellogg, D. R. and Alberts, B. M. (1993). Drosophila gamma-tubulin is part of a complex containing two previously identified centrosomal MAPs. *J Cell Biol* **121**, 823-835.

Rattner, J. B. and Phillips, S. G. (1973). Independence of centriole formation and DNA synthesis. *J Cell Biol* **57**, 359-372.

Rebollo, E. and Gonzalez, C. (2000). Visualizing the spindle checkpoint in Drosophila spermatocytes. *EMBO Rep* **1**, 65-70.

Rebollo, E., Llamazares, S., Reina, J. and Gonzalez, C. (2004). Contribution of noncentrosomal microtubules to spindle assembly in Drosophila spermatocytes. *PLoS Biol* **2**, E8.

Rieder, C. L. (2005). Kinetochore fiber formation in animal somatic cells: dueling mechanisms come to a draw. *Chromosoma* **114**, 310-318.

Rieder, C. L. B., G. G. (1982). The Centrosome Cycle in Ptk2 Cells - Asymmetric Distribution and Structural-Changes in the Pericentriolar Material. *Biology of the Cell* **44**, 117-132.

Rodrigues-Martins, A., Riparbelli, M., Callaini, G., Glover, D. M. and Bettencourt-Dias, M. (2007a). Revisiting the role of the mother centriole in centriole biogenesis. *Science* **316**, 1046-1050.

Rodrigues-Martins, A., Bettencourt-Dias, M., Riparbelli, M., Ferreira, C., Ferreira, I., Callaini, G. and Glover, D. M. (2007b). DSAS-6 organizes a tube-like centriole precursor, and its absence suggests modularity in centriole assembly. *Curr Biol* **17**, 1465-1472.

Ruchaud, S., Carmena, M. and Earnshaw, W. C. (2007). Chromosomal passengers: conducting cell division. *Nat Rev Mol Cell Biol* **8**, 798-812.

Ruiz, F., Garreau de Loubresse, N., Klotz, C., Beisson, J. and Koll, F. (2005). Centrin deficiency in Paramecium affects the geometry of basal-body duplication. *Curr Biol* **15**, 2097-2106.

Satir, P. and Christensen, S. T. (2007). Overview of structure and function of mammalian cilia. *Annu Rev Physiol* **69**, 377-400.

Schafer, M., Nayernia, K., Engel, W. and Schafer, U. (1995). Translational control in spermatogenesis. *Dev Biol* **172**, 344-352.

Schmidt, T. I., Kleylein-Sohn, J., Westendorf, J., Le Clech, M., Lavoie, S. B., Stierhof, Y. D. and Nigg, E. A. (2009). Control of centriole length by CPAP and CP110. *Curr Biol* **19**, 1005-1011.

Scholey, J. M. and Anderson, K. V. (2006). Intraflagellar transport and cilium-based signaling. *Cell* **125**, 439-442.

Schuh, M. and Ellenberg, J. (2007). Self-organization of MTOCs replaces centrosome function during acentrosomal spindle assembly in live mouse oocytes. *Cell* **130**, 484-498.

Shimamura, M., Brown, R. C., Lemmon, B. E., Akashi, T., Mizuno, K., Nishihara, N., Tomizawa, K., Yoshimoto, K., Deguchi, H., Hosoya, H. et al. (2004). Gamma-tubulin in basal land plants: characterization, localization, and implication in the evolution of acentriolar microtubule organizing centers. *Plant Cell* **16**, 45-59.

- Singla, V., Romaguera-Ros, M., Garcia-Verdugo, J. M. and Reiter, J. F.** (2010). Ofd1, a human disease gene, regulates the length and distal structure of centrioles. *Dev Cell* **18**, 410-424.
- Snyder, J. A. and McIntosh, J. R.** (1975). Initiation and growth of microtubules from mitotic centers in lysed mammalian cells. *J Cell Biol* **67**, 744-760.
- Sorokin, S.** (1962). Centrioles and the formation of rudimentary cilia by fibroblasts and smooth muscle cells. *J Cell Biol* **15**, 363-377.
- Stearns, T. and Kirschner, M.** (1994). In vitro reconstitution of centrosome assembly and function: the central role of gamma-tubulin. *Cell* **76**, 623-637.
- Stemm-Wolf, A. J., Morgan, G., Giddings, T. H., Jr., White, E. A., Marchione, R., McDonald, H. B. and Winey, M.** (2005). Basal body duplication and maintenance require one member of the Tetrahymena thermophila centrin gene family. *Mol Biol Cell* **16**, 3606-3619.
- Stevens, N. R., Dobbelaere, J., Brunk, K., Franz, A. and Raff, J. W.** (2010). Drosophila Ana2 is a conserved centriole duplication factor. *J Cell Biol* **188**, 313-323.
- Sullivan, W. and Theurkauf, W. E.** (1995). The cytoskeleton and morphogenesis of the early Drosophila embryo. *Curr Opin Cell Biol* **7**, 18-22.
- Theurkauf, W. E. and Hawley, R. S.** (1992). Meiotic spindle assembly in Drosophila females: behavior of nonexchange chromosomes and the effects of mutations in the nod kinesin-like protein. *J Cell Biol* **116**, 1167-1180.
- Tokuyasu, K. T.** (1975). Dynamics of spermiogenesis in Drosophila melanogaster. VI. Significance of "onion" nebenkern formation. *J Ultrastruct Res* **53**, 93-112.
- Trieselmann, N., Armstrong, S., Rauw, J. and Wilde, A.** (2003). Ran modulates spindle assembly by regulating a subset of TPX2 and Kid activities including Aurora A activation. *J Cell Sci* **116**, 4791-4798.

- Tseng, B. S., Tan, L., Kapoor, T. M. and Funabiki, H.** (2010). Dual detection of chromosomes and microtubules by the chromosomal passenger complex drives spindle assembly. *Dev Cell* **18**, 903-912.
- Tsou, M. F. and Stearns, T.** (2006a). Controlling centrosome number: licenses and blocks. *Curr Opin Cell Biol* **18**, 74-78.
- Tsou, M. F. and Stearns, T.** (2006b). Mechanism limiting centrosome duplication to once per cell cycle. *Nature* **442**, 947-951.
- Uehara, R., Nozawa, R. S., Tomioka, A., Petry, S., Vale, R. D., Obuse, C. and Goshima, G.** (2009). The augmin complex plays a critical role in spindle microtubule generation for mitotic progression and cytokinesis in human cells. *Proc Natl Acad Sci U S A* **106**, 6998-7003.
- Varmark, H.** (2004). Functional role of centrosomes in spindle assembly and organization. *J Cell Biochem* **91**, 904-914.
- Varmark, H., Llamazares, S., Rebollo, E., Lange, B., Reina, J., Schwarz, H. and Gonzalez, C.** (2007). Asterless is a centriolar protein required for centrosome function and embryo development in *Drosophila*. *Curr Biol* **17**, 1735-1745.
- Veland, I. R., Awan, A., Pedersen, L. B., Yoder, B. K. and Christensen, S. T.** (2009). Primary cilia and signaling pathways in mammalian development, health and disease. *Nephron Physiol* **111**, p39-53.
- Vorobjev, I. A. and Chentsov Yu, S.** (1982). Centrioles in the cell cycle. I. Epithelial cells. *J Cell Biol* **93**, 938-949.
- Walczak, C. E. and Heald, R.** (2008). Mechanisms of mitotic spindle assembly and function. *Int Rev Cytol* **265**, 111-158.
- Wang, P. J. and Pan, J.** (2007). The role of spermatogonially expressed germ cell-specific genes in mammalian meiosis. *Chromosome Res* **15**, 623-632.
- Wang, Z. and Mann, R. S.** (2003). Requirement for two nearly identical TGIF-related homeobox genes in *Drosophila* spermatogenesis. *Development* **130**, 2853-2865.

- Wasteney, G. O. and Ambrose, J. C.** (2009). Spatial organization of plant cortical microtubules: close encounters of the 2D kind. *Trends Cell Biol* **19**, 62-71.
- Wheatley, D. N., Wang, A. M. and Strugnell, G. E.** (1996). Expression of primary cilia in mammalian cells. *Cell Biol Int* **20**, 73-81.
- White-Cooper, H.** (2010). Molecular mechanisms of gene regulation during Drosophila spermatogenesis. *Reproduction* **139**, 11-21.
- White-Cooper, H. and Bausek, N.** (2010). Evolution and spermatogenesis. *Philos Trans R Soc Lond B Biol Sci* **365**, 1465-1480.
- White-Cooper, H., Alphey, L. and Glover, D. M.** (1993). The cdc25 homologue twine is required for only some aspects of the entry into meiosis in Drosophila. *J Cell Sci* **106 (Pt 4)**, 1035-1044.
- White-Cooper, H., Schafer, M. A., Alphey, L. S. and Fuller, M. T.** (1998). Transcriptional and post-transcriptional control mechanisms coordinate the onset of spermatid differentiation with meiosis I in Drosophila. *Development* **125**, 125-134.
- White-Cooper, H., Leroy, D., MacQueen, A. and Fuller, M. T.** (2000). Transcription of meiotic cell cycle and terminal differentiation genes depends on a conserved chromatin associated protein, whose nuclear localisation is regulated. *Development* **127**, 5463-5473.
- Wittmann, T., Wilm, M., Karsenti, E. and Vernos, I.** (2000). TPX2, A novel xenopus MAP involved in spindle pole organization. *J Cell Biol* **149**, 1405-1418.
- Wong, C. and Stearns, T.** (2003). Centrosome number is controlled by a centrosome-intrinsic block to reduplication. *Nat Cell Biol* **5**, 539-544.
- Wong, J. and Fang, G.** (2006). HURP controls spindle dynamics to promote proper interkinetochore tension and efficient kinetochore capture. *J Cell Biol* **173**, 879-891.

- Wuhr, M., Chen, Y., Dumont, S., Groen, A. C., Needleman, D. J., Salic, A. and Mitchison, T. J.** (2008). Evidence for an upper limit to mitotic spindle length. *Curr Biol* **18**, 1256-1261.
- Zhai, Y. and Borisy, G. G.** (1994). Quantitative determination of the proportion of microtubule polymer present during the mitosis-interphase transition. *J Cell Sci* **107 (Pt 4)**, 881-890.
- Zheng, Y., Wong, M. L., Alberts, B. and Mitchison, T.** (1995). Nucleation of microtubule assembly by a gamma-tubulin-containing ring complex. *Nature* **378**, 578-583.

Ramona Lattao

LIST OF PUBLICATIONS

- **Lattao, R., Bonaccorsi, S., Guan, X., Wasserman, S., and Gatti, M.** (2011) Tubby-tagged balancers for the *Drosophila* X and second chromosomes. *Fly* (Austin). 2011 Oct 1;5(4).

- **Lattao, R., Bonaccorsi, S., and Gatti, M.** Giant meiotic spindles in males from *Drosophila* species with giant sperm tails. *J Cell Sci.* *in press*.

Meeting abstracts:

- **Maurizio Gatti, Silvia Bonaccorsi, Ramona Lattao.** Giant meiotic spindles in males from *Drosophila* species with giant sperm tails. 51st Annual *Drosophila* Research Conference. Washington DC (USA) 7-11 april 2010

- **Ramona Lattao, Silvia Bonaccorsi and Maurizio Gatti.** The *fragile centrioles (fract)* gene is required for the maintenance of centriole integrity during *Drosophila* male meiosis. 2011 ASCB Annual Meeting. Denver, CO (USA) 3-7 december 2011

Ramona Lattao

ACKNOWLEDGEMENTS

I am grateful to Professor Silvia Bonaccorsi and Professor Maurizio Gatti who gave me the opportunity to work with them and for their important support throughout this work.

I wish to thank Dr. Patrizia Lavia, PhD (Institute of Molecular Biology and Pathology of the National Research Council in Rome, Italy) for her detailed review, constructive comments and excellent advice during the preparation of this thesis.

I also wish to thank my colleagues of Gatti lab.